

Piperazine Imidazo[1,5-*a*]quinoxaline Ureas as High-Affinity GABA_A Ligands of Dual Functionality[†]

E. Jon Jacobsen,^{*,‡} Lindsay S. Stelzer,[‡] Ruth E. TenBrink,[‡] Kenneth L. Belonga,[‡] Donald B. Carter,[§] Haesook K. Im,[§] Wha Bin Im,[§] Vimala H. Sethy,[§] Andy H. Tang,[§] Philip F. VonVoigtlander,[§] James D. Petke,^{||} Wei-Zhu Zhong,[⊥] and John W. Mickelson[∇]

Departments of Structural, Analytical and Medicinal Chemistry, Central Nervous System Diseases Research, Computer Aided Drug Discovery, and Pharmacokinetics and Bioanalysis Research, Upjohn Laboratories, Pharmacia & Upjohn, Inc., Kalamazoo, Michigan 49001

Received February 27, 1998

A series of imidazo[1,5-*a*]quinoxaline piperazine ureas appended with a *tert*-butyl ester side chain at the 3-position was developed. Analogues within this series have high affinity for the γ -aminobutyric acid A (GABA_A)/benzodiazepine receptor complex with efficacies ranging from inverse agonists to full agonists. Many analogues were found to be partial agonists as indicated by [³⁵S]TBPS and Cl⁻ current ratios. Uniquely, a number of these analogues were found to have a bell-shaped dose–response profile in the $\alpha_1\beta_2\gamma_2$ subtype as determined by whole cell patch-clamp technique, where *in vitro* efficacy was found to decrease with increasing drug concentration. Many of the compounds from this series were effective in antagonizing metrazole-induced seizures, consistent with anticonvulsant and possibly anxiolytic activity. Additionally, several analogues were also effective in lowering cGMP levels (to control values) after applied stress, also consistent with anxiolytic-like properties. The most effective compounds in these screens were also active in animal models of anxiety such as the Vogel and Geller assays. The use of the piperazine substituent allowed for excellent drug levels and a long duration of action in the central nervous system for many of the quinoxalines, as determined by *ex vivo* assay. Pharmacokinetic analysis of several compounds indicated excellent oral bioavailability and a reasonable half-life in rats. From this series emerged two partial agonists (**55**, **91**) which had good activity in anxiolytic models, acceptable pharmacokinetics, and minimal benzodiazepine-type side effects.

The action of γ -aminobutyric acid (GABA) on the GABA_A chloride ion channel complex controls the excitability of many central nervous system (CNS) pathways.¹ Numerous chemical classes have binding sites on this macromolecular ionophore, including the benzodiazepines, neurosteroids, and barbiturates. Compounds which interact with the benzodiazepine receptor (BzR) and allosterically modulate the action of GABA on neuronal chloride flux have a continuum of intrinsic activity,² ranging from full agonists (anxiolytic, hypnotic, and anticonvulsant agents) through antagonists to inverse agonists (proconvulsant and anxiogenic agents). Partial agonists lie within this continuum and may have reduced benzodiazepine-mediated side effects such as physical dependence, amnesia, oversedation (anxiolytics), and muscle relaxation.³ The discovery and characterization of partial agonist ligands have been reported by several research groups.^{4–10} Furthermore, recent molecular biology studies have demonstrated that several different receptor subunits (α , β , γ , δ) combine to form the GABA_A receptor complex,¹¹ with at least three to four native receptor subtypes identified thus

far.¹² Subtype selective ligands may also allow for the discrimination between useful anxiolytic or hypnotic activity and overt side effects, and as such they are a topic of current research.

We recently reported on an imidazo[1,5-*a*]quinoxaline urea **1** (PNU-91571, Figure 1) which was a partial agonist *in vitro* ($\alpha_1\beta_2\gamma_2$ and $\alpha_3\beta_2\gamma_2$ subtypes) and displayed useful activity in anxiolytic models, yet lacked typical benzodiazepine-type side effects such as physical dependence and ethanol potentiation.¹³ Unfortunately this analogue contained a 5'-cyclopropyl-1',2',4'-oxadiazole group at the 3-position, which in the case of **2** (pandiplon, PNU-78875)^{9a} is metabolized to release cyclopropanecarboxylic acid, leading to an increase in serum triglycerides.¹⁴ Although **1** had a different metabolic profile than **2**, concerns over possible degradation of the oxadiazole group to release cyclopropane carboxylic acid precluded further development of this compound.

Efforts to replace the oxadiazole with other aromatic groups such as phenyl,¹⁵ oxazole, or isoxazole were successful with respect to maintaining excellent binding affinity; however, unacceptable benzodiazepine (BzD) side effects were typically observed. While the use of an ester substituent at the 3-position also maintained affinity, intrinsic activity was notably decreased. In our exploration of the 3-phenyl series,¹⁵ the use of a *cis*-2,6-dimethylpiperazine as the urea substituent was found to dramatically improve CNS penetration and duration of action (by *ex vivo* assay) as compared to other ureas

[†]A portion of this material was presented at the Winter Conference on Medicinal and Bioorganic Chemistry, Steamboat Springs, CO, January 28, 1995.

[‡] Department of Structural, Analytical and Medicinal Chemistry.

[§] Department of Central Nervous Diseases System Research.

^{||} Department of Computer Aided Drug Discovery.

[⊥] Department of Pharmacokinetics and Bioanalysis Research.

[∇] Present address: 3M Pharmaceuticals, 3M Center Bldg., St. Paul, MN 55144-1000.

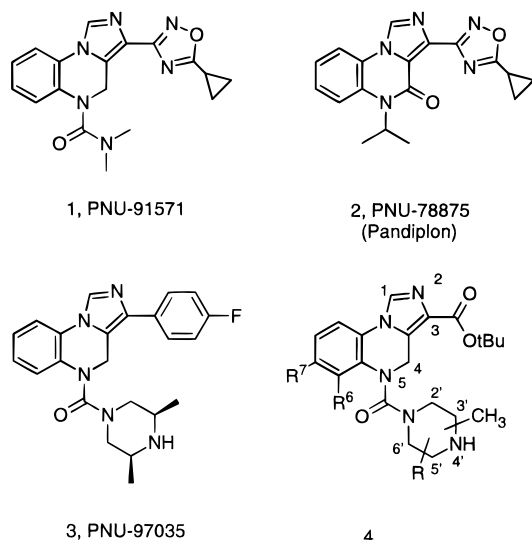


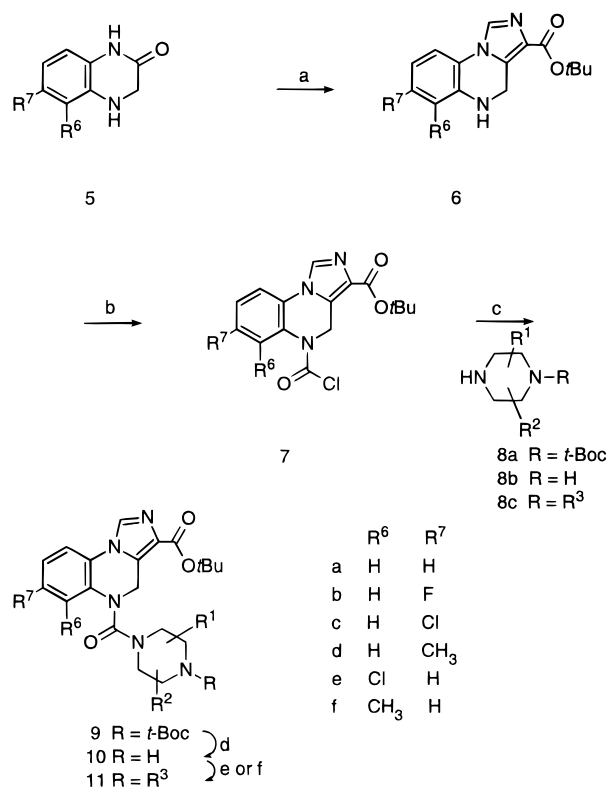
Figure 1. Quinoxalines 1–4.

lacking a basic nitrogen. More importantly, compounds such as **3** (PNU-97035, Figure 1) were found to display biphasic efficacy by *in vitro* measurement, becoming increasingly antagonistic with increasing drug concentration. While the observed biphasic efficacy did not serve to minimize side effects such as physical dependence, which in this series was severe, this unique property was worthy of further evaluation. With proper adjustment of intrinsic activity, a therapeutic agent with biphasic efficacy similar to that observed for **3** would serve to limit its own agonistic effects over a wide dose range, potentially minimizing its abuse potential. In this paper we report on the use of a *tert*-butyl ester substituent at the 3-position which, in combination with a *C*-methyl piperazine urea (i.e., **4**, Figure 1), provides for partial agonist activity. Furthermore, several analogues were identified which have excellent activity in anxiolytic models, minimal BzD-type side effects, and acceptable pharmacokinetic properties.

Chemistry

The general synthesis of the *tert*-butyl imidazo[1,5-*a*]quinoxaline carboxylates was carried out in a fashion similar to that of the oxadiazoles reported previously^{13,16} and is shown in Scheme 1. Imidazo-annulation of quinoxalin-2-one (**5**),^{13,16} via the intermediate enol phosphonate using *tert*-butyl isocynoacetate, provided imidazo[1,5-*a*]quinoxaline **6** in 60–80% yield. The carbamoyl chloride **7** was formed by reaction of **6** with phosgene or triphosgene in the presence of Hunig's base. This intermediate (**7**) could either be isolated or, more frequently, reacted *in situ* with the desired piperazine **8a–8c** to give ureas **9**, **10**, and **11**, respectively. Protection of the piperazine (**8a** vs **8b**) was usually not necessary for the *cis*-2,6-dimethylpiperazine reagent, with excellent yields usually achieved. For less bulky piperazines, regioisomeric or bis-addition to **7** often occurred. These side reactions could be avoided (partially) through the use of a large excess of the desired piperazine. For example, in the case of **76** the use of 1.0 equiv of 2-methylpiperazine (**8b**, R¹ = Me) provided only a 19% yield of the urea. The yield could be significantly improved (64%) by the use of 10 equiv of the piperazine reagent. Nonetheless, for the more

Scheme 1^a

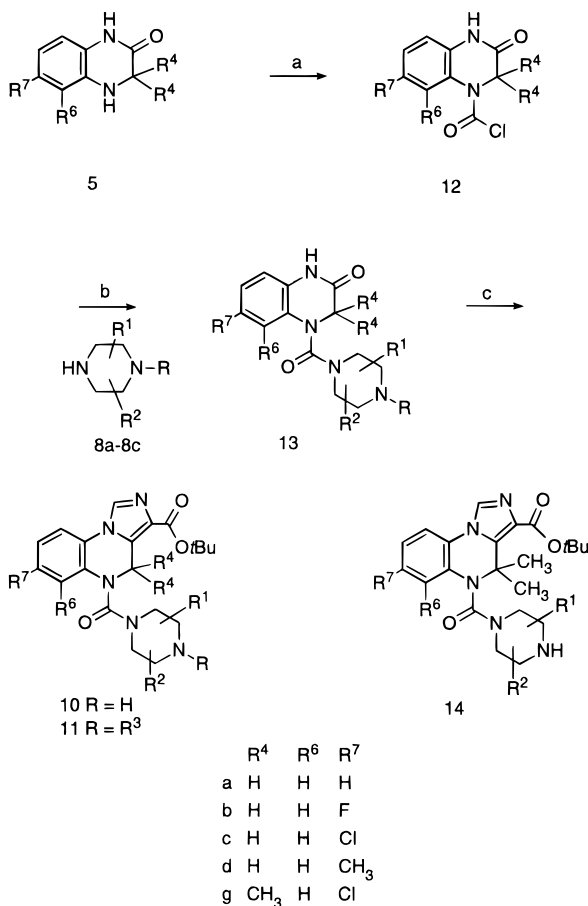


^a Reagents: (a) ^tBuOH, THF; diethyl chlorophosphate; ^tBuOK, CNCH₂CO₂^tBu; (b) phosgene or triphosgene, Et₃N/Pr₂, CH₂Cl₂; (c) **8a–8c**, Et₃N/Pr₂, CH₂Cl₂; (d) TFA, CH₂Cl₂, 0 °C; (e) R³CHO, NaCNBH₃, MeOH; (f) R³Cl, Et₃N/Pr₂, CH₂Cl₂.

elaborated piperazines, a *t*-Boc protecting group (**8a**, **9**) was utilized which was easily removed using TFA to give **10**, with no cleavage of the *tert*-butyl ester observed. The introduction of an *N*-alkyl group in **10** to give piperazine **11** (R³ = alkyl) was generally carried out by the reductive amination procedure of Borch.¹⁷ Alternatively, the *N*-alkyl group was incorporated in piperazine **8c** (R³ = alkyl) to give **11** directly (**7** → **11**). Simple acylation of **10** provided analogues **71** and **72**.

An alternative sequence, particularly useful for the synthesis of *gem*-4,4-dimethylimidazo[1,5-*a*]quinoxaline **14**, is shown in Scheme 2. Conversion of **5** to piperazine urea **13** via the carbamoyl chloride proceeded uneventfully. As described above, reaction of the enol phosphonate of **13** with *tert*-butyl isocynoacetate provided **10** or **11** in good yield. Elaboration of **10** to the desired quinoxaline **11**, if desired, was carried out as detailed in Scheme 1. This sequence was critical for the synthesis of **57** and **58**, which contained *gem*-dimethyl groups (i.e., **14**) at the 4-position.

The synthesis of the quinoxalin-2-one starting materials **5a–5g** was carried out as previously described.^{13,16} Incorporation of a trifluoromethyl group into this template at the 7-position was accomplished as shown in Scheme 3. Reaction of 2-chloro-5-trifluoromethyl-nitrobenzene **15** with dibenzylamine provided **16** in excellent yield. Reduction of **16** using Raney nickel provided aniline **17**, which was alkylated with ethyl bromoacetate in neat Hunig's base to give **18** in a reasonable 70% yield. Hydrogenation using Pearlman's catalyst provided a 97% yield of the desired quinoxaline, which was isolated in its enol form **19** due to the

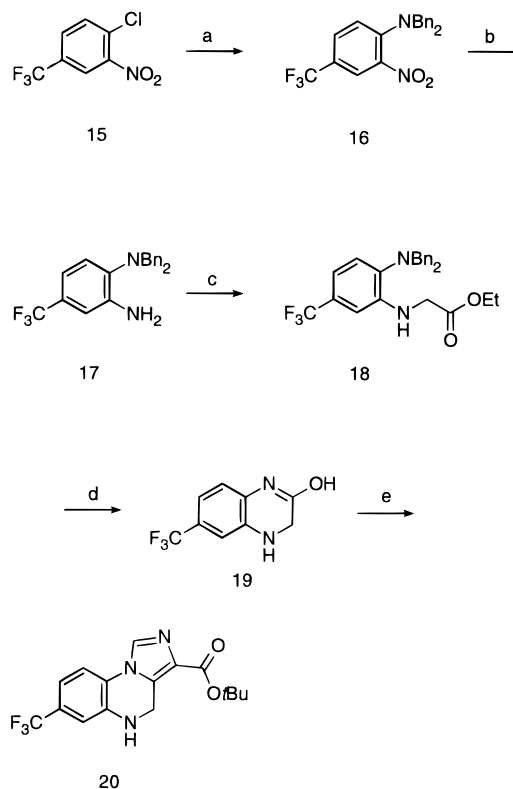
Scheme 2^a

^a Reagents: (a) phosgene, EtN^tPr₂, CH₂Cl₂; (b) **8a–8c**, EtN^tPr₂, CH₂Cl₂; (c) ^tBuOK, THF; diethyl chlorophosphate; CNCH₂CO₂^tBu, ^tBuOK.

electron-withdrawing effects of the trifluoromethyl group. Cyclization of **19** under standard conditions provided the desired imidazo[1,5-a]quinoxaline **20**.

A number of noncommercial piperazines (Figure 2) were synthesized according to literature precedent, with minor protecting group manipulation, if necessary. These piperazines and bicyclo-derived analogues **21**,¹⁸ **22**,¹⁹ **23**,²⁰ **24**,²¹ **25**,²² **26**,²² **27**,²³ and **28**²⁴ were prepared to fully explore the structure–activity relationship (SAR) of the urea substituent. Piperazine **32** (1-isopropyl-*cis*-2,6-dimethylpiperazine) was synthesized by straightforward chemistry as shown in Scheme 4.

The chiral 3,5-methylated piperazine urea analogues (**89–100**) were synthesized by one of two methods. As illustrated in Scheme 1, reaction of carbamoyl chloride **7** with the individual enantiomers of 2-methylpiperazine²⁵ or *trans*-2,6-dimethylpiperazine²⁵ provided the desired quinoxaline ureas **10** directly. An alternative approach using an intramolecular Mitsunobu reaction²⁶ was also developed as shown in Scheme 5. Following our previously outlined chemistry,²⁵ but without protecting groups, the desired antipode of Boc-alanine **33** was converted to amides **34A** and **34B** by reaction of the CDI-intermediate with ethanolamine or 1-amino-2-propanol (*R*-shown). Reduction of **34A** or **34B** with borane–methyl sulfide complex and hydrolysis of the intermediate borane adduct with aqueous HCl followed by aqueous potassium hydroxide provided amines **35A** and **35B** in good yield. Reaction of either of these amines

Scheme 3^a

^a Reagents: (a) Bn₂NH, EtN^tPr₂, 140 °C; (b) H₂NHNH₂·H₂O, Raney nickel, EtOH; (c) BrCH₂CO₂Et, EtN^tPr₂, 120 °C; (d) Pd(OH)₂, H₂, EtOH; (e) ^tBuOK, THF; diethyl chlorophosphate; CNCH₂CO₂^tBu, ^tBuOK.

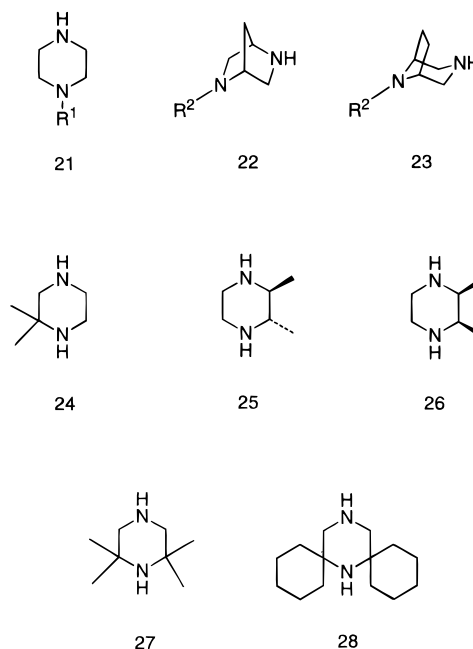
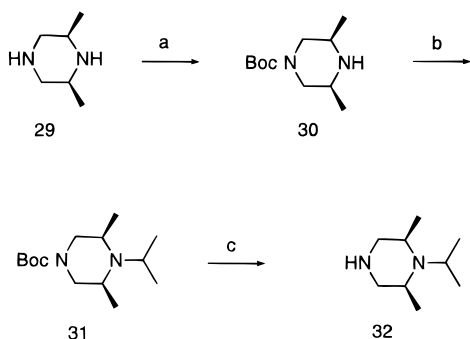
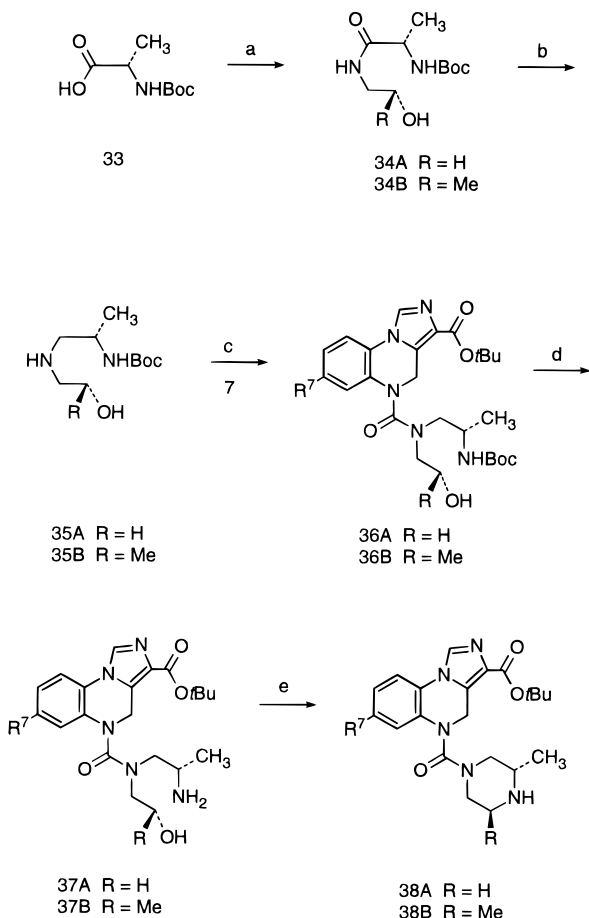


Figure 2. Selected piperazine intermediates.

with carbamoyl chloride **7** provided amides **36A** and **36B**, which were deprotected with TFA to give amino alcohols **37A** and **37B**. Intramolecular cyclization of **37A** and **37B** using Mitsunobu conditions provided the desired piperazines **38A** and **38B**. This latter strategy, which avoided protecting group manipulation, was quite efficient and provided the 3-methyl- and *trans*-3,5-dimethylpiperazines in >98% ee as determined by HPLC

Scheme 4^a

^a Reagents: (a) di-*tert*-butyl dicarbonate, CH₂Cl₂; (b) (CH₃)₂CHCH₂I, K₂CO₃, CH₃CN; (c) TFA, CH₂Cl₂, 0 °C.

Scheme 5^a

^a Reagents: (a) CDI, CH₂Cl₂; ethanolamine or (*R*)-1-amino-2-propanol; (b) BH₃·DMS, THF; 10% HCl; KOH, THF, H₂O, reflux; (c) **7**, EtNⁱPr₂, CH₂Cl₂; (d) TFA, CH₂Cl₂, 0 °C; (e) DEAD, PPh₃, THF.

or ¹H NMR analysis.²⁷ Table 1 highlights the physical data and methods used for the synthesis of the imidazo-[1,5-*a*]quinoxaline piperazines as well those for a few simple urea analogues.

Results and Discussion

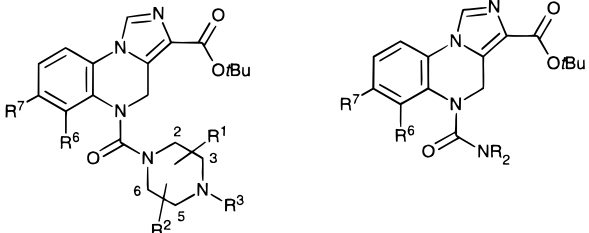
The piperazine quinoxalines were initially evaluated for binding affinity and *in vitro* efficacy. Binding affinity for the benzodiazepine receptor in rat cortical membranes was determined by competition experiments with radiolabeled [³H]flunitrazepam.²⁸ Selected analogues were also evaluated for affinity to individual

benzodiazepine receptor subtypes to assess binding selectivity.^{29,30} Classical benzodiazepines interact with the $\alpha_1\beta_2\gamma_2$, $\alpha_2\beta_2\gamma_2$, $\alpha_3\beta_2\gamma_2$, and $\alpha_5\beta_2\gamma_2$ subtypes with nearly equal affinity,³¹ while atypical BzR ligands such as Cl 218872 and Zolpidem have moderate selectivity for the $\alpha_1\beta_2\gamma_2$ subtype.^{4a,31} In contrast, classical benzodiazepines do not interact with the $\alpha_6\beta_2\gamma_2$ subtype located in cerebellar granule cells, whereas ligands such as Ro 15-4513 and (*RS*)-1-(5-cyclopropyl-1,2,4-oxadiazol-3-yl)-12,12a-dihydroimidazo[1,5-*a*]pyrrolo[2,1-*c*]quinoxalin-10(11*H*)-one (PNU-89267) have high affinity for this subtype.^{16,32} The search for selective ligands for these subtypes, as well as the elucidation of their function, remains an important goal in this area.

Two different methods were utilized to evaluate the *in vitro* efficacy of these compounds. The TBPS shift ratio³³ was determined for each analogue by measuring its effect on *tert*-butylbicyclophosphorothionate (TBPS) binding to the picrotoxin convulsant site on the GABA_A chloride complex. Differences in TBPS binding presumably occur due to conformational changes in the chloride ionophore as it is allosterically modulated by the binding of the test compound to the benzodiazepine receptor. As reported previously,¹³ the resultant value (expressed as a ratio of that for the test drug to that of diazepam) is 1 for a full agonist and 0 for an antagonist, with negative values for inverse agonists. Partial agonists have values intermediate between 0 and 1. A more direct measure of *in vitro* efficacy was determined by a Cl⁻ current assay.³³⁻³⁵ The synaptic chloride conductance resulting from the activation of the GABA_A receptor complex by GABA is modulated by ligands acting at the benzodiazepine receptor. Full agonists increase Cl⁻ current and antagonists have no effect, while inverse agonists decrease ion flow. The test compounds are compared to diazepam and thus have a numerical scale like the TBPS assay. In general, the chloride current assay provides a more direct measure of efficacy as it is run in a single subtype ($\alpha_1\beta_2\gamma_2$), whereas the TBPS shift ratio is determined across the native population. Results from these assays are often different due to the heterogeneity of the native GABA_A receptor population. Furthermore, as the Cl⁻ current and TBPS assays are also run at different drug concentrations, biphasic piperazine ureas¹⁵ such as **3** (Figure 1) often display dramatically different values. Many of the urea analogues were evaluated at two different drug concentrations in the Cl⁻ current assay in order to assess possible biphasic effects. In addition, as benzodiazepine ligands are known to display efficacy selectivity in different receptor subtypes,³⁶ selected analogues were screened for intrinsic efficacy in the $\alpha_1\beta_2\gamma_2$ and $\alpha_3\beta_2\gamma_2$ subtypes.

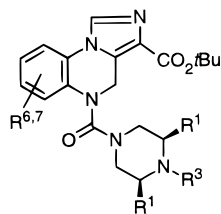
To provide a quick measure of *in vivo* efficacy, most analogues were evaluated for their ability to antagonize metrazole-induced seizures (clonic and tonic).³⁷ While a direct measure of anticonvulsant activity, this assay is also predictive of anxiolytic properties, as standard full agonist benzodiazepine agents such as diazepam, alprazolam, and zolpidem (and partial agonists **2**, bretazenil, and abecarnil) are extremely effective (ED₅₀'s 0.17–4.5 mg/kg). The results of the flunitrazepam,

Table 1. Physical Data for Imidazo[1,5-a]quinoxaline Ureas, Carbamates, and Amides



compd	R ¹	R ²	R ³	R ⁶	R ⁷	mp (°C)	method	yield (%)	formula	anal.
39	H	H	H	H	H	260–261	A	70	C ₂₀ H ₂₅ N ₅ O ₃ ·(HCl)·(H ₂ O) ₃	C, H, N
40	<i>cis</i> -3,5-dimethyl		H	H	H	186–187	A	87	C ₂₂ H ₂₉ N ₅ O ₃	C, H, N
41	<i>cis</i> -3,5-dimethyl	Me	H	H	H	190–192	B	78	C ₂₃ H ₃₁ N ₅ O ₃	C, H, N
42	<i>cis</i> -3,5-dimethyl	H	H	H	F	166–168	E	68	C ₂₂ H ₂₈ N ₅ O ₃ F	C, H, N
43	<i>cis</i> -3,5-dimethyl	Me	H	H	F	154–156	B	53	C ₂₃ H ₃₀ N ₅ O ₃ F	C, H, N ^d
44	H	H	H	H	Cl	187–188	A	59	C ₂₀ H ₂₄ N ₅ O ₃ Cl	C, H, N, Cl
45	H	H	Me	H	Cl	169–171	E	48	C ₂₁ H ₂₆ N ₅ O ₃ Cl	C, H, N, Cl
46	<i>cis</i> -3,5-dimethyl	H	H	H	Cl	200.5–201	A	80	C ₂₂ H ₂₈ N ₅ O ₃ Cl·(C ₄ H ₈ O ₂) _{1/4}	C, H, N, Cl
47	<i>cis</i> -3,5-dimethyl	Me	H	H	Cl	172–173	B	92	C ₂₃ H ₃₀ N ₅ O ₃ Cl·(H ₂ O) _{1/2}	C, H, N, Cl
48	<i>cis</i> -3,5-dimethyl	H	H	Cl	H	>300	A	86	C ₂₂ H ₂₈ N ₅ O ₃ Cl·(H ₂ O) _{1/4}	C, H, N, Cl
49	<i>cis</i> -3,5-dimethyl	Me	Cl	H	H	221–222	B	88	C ₂₃ H ₃₀ N ₅ O ₃ Cl·(H ₂ O) _{3/4}	C, H, N, Cl
50	H	H	H	H	Me	214–214.5	A	59	C ₂₁ H ₂₇ N ₅ O ₃ ·(H ₂ O) _{1/8}	C, H, N
51	<i>cis</i> -3,5-dimethyl	H	H	H	Me	188–190	E	69	C ₂₃ H ₃₁ N ₅ O ₃ ·(H ₂ O) _{1/5}	C, H, N
52	<i>cis</i> -3,5-dimethyl	Me	H	H	Me	200–201	E	73	C ₂₄ H ₃₃ N ₅ O ₃	C, H, N
53	<i>cis</i> -3,5-dimethyl	H	Me	H	H	212–213.5	A	74	C ₂₃ H ₃₁ N ₅ O ₃ ·(H ₂ O) _{1/4}	C, H, N
54	<i>cis</i> -3,5-dimethyl	Me	Me	H	H	208–210	B	82	C ₂₄ H ₃₃ N ₅ O ₃	C, H, N
55	<i>cis</i> -3,5-dimethyl	H	H	H	CF ₃	184–186	A	82	C ₂₃ H ₂₈ N ₅ O ₃ F ₃	C, H, N
56	<i>cis</i> -3,5-dimethyl	Me	H	H	CF ₃	177–181	B	81	C ₂₄ H ₃₀ N ₅ O ₃ F ₃ ·(H ₂ O) _{2/3}	C, H, N
57 ^b	<i>cis</i> -3,5-dimethyl	H	H	H	Cl	171–175	E	47	C ₂₄ H ₃₂ N ₅ O ₃ Cl	C, H, N, Cl ^c
58 ^b	<i>cis</i> -3,5-dimethyl	Me	H	H	Cl	200–201	E	30	C ₂₅ H ₃₄ N ₅ O ₃ Cl	C, H, N, Cl
59		NR ₂ = NMe ₂	H	H	H	184–186	E	53	C ₁₈ H ₂₂ N ₄ O ₃	C, H, N
60		NR ₂ = piperidine	H	H	H	167–167.5	E	66	C ₂₁ H ₂₆ N ₄ O ₃	C, H, N
61		NR ₂ = morpholine	H	H	H	205–206	E	62	C ₂₀ H ₂₄ N ₄ O ₄	C, H, N
62		NR ₂ = NMe ₂	H	H	Cl	210–211.5	E	48	C ₁₈ H ₂₁ N ₄ O ₃ Cl	C, H, N, Cl
63		NR ₂ = pyrrolidine	H	H	Cl	194–196	E	47	C ₂₀ H ₂₃ N ₄ O ₃ Cl·(C ₄ H ₈ O ₂) _{1/4}	C, H, N, Cl
64	H	H	^t Bu	H	Cl	187.5–189	A	79	C ₂₄ H ₃₂ N ₅ O ₃ Cl	C, H, N, Cl
65	H	H	ⁱ Pr	H	Cl	222–224	A	77	C ₂₃ H ₂₈ N ₅ O ₃ Cl	C, H, N, Cl
66	H	H	2-pyridyl	H	Cl	233–235	A	74	C ₂₅ H ₂₇ N ₆ O ₃ Cl	C, H, N, Cl
67	H	H	CH ₂ CF ₃	H	Cl	225–226	C	84	C ₂₂ H ₂₅ N ₅ O ₃ ClF ₃	C, H, N, Cl
68	<i>cis</i> -3,5-dimethyl	Et	H	H	Cl	127–130	B	64	C ₂₄ H ₃₂ N ₅ O ₃ Cl·(C ₄ H ₈ O ₂) _{1/2} ·(H ₂ O) _{1.33}	C, H, N, Cl
69	<i>cis</i> -3,5-dimethyl	^t Pr	H	H	Cl	186–187	A	96	C ₂₅ H ₃₄ N ₅ O ₃ Cl	C, H, N, Cl
70	<i>cis</i> -3,5-dimethyl	CH ₂ CF ₃	H	H	Cl	211–213	C	95	C ₂₄ H ₂₉ N ₅ O ₃ ClF ₃	C, H, N, Cl
71	<i>cis</i> -3,5-dimethyl	COCH ₃	H	H	Cl	154–154.5	87	C ₂₄ H ₃₀ N ₅ O ₄ Cl	C, H, N, Cl	
72	<i>cis</i> -3,5-dimethyl	SO ₂ Me	H	H	Cl	156–156.5	62	C ₂₃ H ₃₀ N ₅ O ₅ ClS·(CH ₂ Cl ₂) _{1/10}	C, H, N, ^d Cl, S	
73	<i>cis</i> -2,6-dimethyl	H	H	F	F	136–137.5	D	60	C ₂₂ H ₂₈ N ₅ O ₃ F	C, H, N
74	<i>cis</i> -2,6-dimethyl	Me	H	F	F	152–153	B	64	C ₂₃ H ₃₀ N ₅ O ₃ F	C, H, N
75	<i>cis</i> -2,6-dimethyl	Me	H	H	Cl	160–161	E	31	C ₂₃ H ₃₀ N ₅ O ₃ Cl	C, H, N, Cl
76	3-CH ₃	H	H	H	Cl	169–172	A	19 (64) ^e	C ₂₁ H ₂₆ N ₅ O ₃ Cl	C, H, N, Cl
77	<i>trans</i> -3,5-dimethyl	H	H	H	Cl	128–130	C	36	C ₂₂ H ₂₈ N ₅ O ₃ Cl·(H ₂ O) _{4/5}	C, H, N, Cl
78	<i>trans</i> -2,5-dimethyl	H	H	H	Cl	186–187	A	56	C ₂₂ H ₂₈ N ₅ O ₃ Cl·(C ₃ H ₄ O ₄)·(H ₂ O) _{2/3}	C, H, N, Cl
79	<i>cis</i> -2,3-dimethyl	H	H	H	Cl	168–169	D	41	C ₂₂ H ₂₈ N ₅ O ₃ Cl	C, H, N, Cl
80	<i>trans</i> -2,3-dimethyl	H	H	H	Cl	164–165	C	30	C ₂₂ H ₂₈ N ₅ O ₃ Cl	C, H, N, Cl
81	3,3-dimethyl	H	H	H	Cl	161–162	C	56	C ₂₂ H ₂₈ N ₅ O ₃ Cl·(H ₂ O) _{1/4}	C, H, N, Cl
82	3,3-dimethyl	Me	H	H	Cl	206–207	B	82	C ₂₃ H ₃₀ N ₅ O ₃ Cl	C, H, N, Cl
83	3,3,5,5-tetramethyl	H	H	H	Cl	140–143	A	71	C ₂₄ H ₃₂ N ₅ O ₃ Cl·(H ₂ O) _{1/4}	C, H, N, Cl
84	bis-spiro-cyclohexyl	H	H	H	Cl	217–220	C	65	C ₃₀ H ₄₀ N ₅ O ₃ Cl·(H ₂ O) _{1/4}	C, H, N, Cl
85		H	H	H	Cl	270–272	D	63	C ₂₁ H ₂₄ N ₅ O ₃ Cl·(H ₂ O)	C, H, N, Cl
86			Me	H	Cl	174–176	C	48	C ₂₂ H ₂₆ N ₅ O ₃ Cl·(H ₂ O) _{1/4}	C, H, N, Cl
87			H	H	Cl	207–210	D	79	C ₂₂ H ₂₆ N ₅ O ₃ Cl·(H ₂ O) _{1/4}	C, H, N, Cl
88			Me	H	Cl	213–216	B	80	C ₂₃ H ₂₈ N ₅ O ₃ Cl	C, H, N, Cl
89	3(<i>S</i>)-Me	H	H	H	Cl	158–160	F	59	C ₂₁ H ₂₆ N ₅ O ₃ Cl·(H ₂ O) _{4/5}	C, H, N, Cl
90	3(<i>R</i>)-Me	H	H	H	Cl	157–159	D	76	C ₂₁ H ₂₆ N ₅ O ₃ Cl·(H ₂ O) _{1/2}	C, H, N, Cl
91	3(<i>S</i>)-Me	5(<i>S</i>)-Me	H	H	Cl	121–125	F	71	C ₂₂ H ₂₈ N ₅ O ₃ Cl·(H ₂ O) _{1/3}	C, H, N, Cl
92	3(<i>R</i>)-Me	5(<i>R</i>)-Me	H	H	Cl	125–127	F	55	C ₂₂ H ₂₈ N ₅ O ₃ Cl·(H ₂ O) _{1/3}	C, H, N, Cl
93	3(<i>S</i>)-Me	H	H	H	Me	161–165	D	59	C ₂₂ H ₂₉ N ₅ O ₃ ·(H ₂ O) _{1/2}	C, H, N
94	3(<i>R</i>)-Me	H	H	H	Me	148–152	D	71	C ₂₂ H ₂₉ N ₅ O ₃ ·(H ₂ O) _{3/5}	C, H, N
95	3(<i>S</i>)-Me	5(<i>S</i>)-Me	H	H	Me	140–144	C	60	C ₂₃ H ₃₁ N ₅ O ₃ ·(H ₂ O) _{1/2}	C, H, N
96	3(<i>R</i>)-Me	5(<i>R</i>)-Me	H	H	Me	127–130	C	67	C ₂₃ H ₃₁ N ₅ O ₃ ·(H ₂ O) _{1/2}	C, H, N
97	3(<i>S</i>)-Me	H	H	H	CF ₃	187–188	D	64	C ₂₂ H ₂₆ N ₅ O ₃ F ₃	C, H, N
98	3(<i>R</i>)-Me	H	H	H	CF ₃	176.5–180.5	D	64	C ₂₂ H ₂₆ N ₅ O ₃ F ₃ ·(H ₂ O) _{1/5}	C, H, N ^c
99	3(<i>S</i>)-Me	5(<i>S</i>)-Me	H	H	CF ₃	151–154	F	52	C ₂₃ H ₂₈ N ₅ O ₃ F ₃ ·(H ₂ O) _{1/2}	C, H, N
100	3(<i>R</i>)-Me	3(<i>R</i>)-Me	H	H	CF ₃	157–158	F	65	C ₂₃ H ₂₈ N ₅ O ₃ F ₃	C, H, N

^a N: calcd, 15.79; found, 15.29. ^b *gem*-4,4-Dimethyl. ^c Cl: calcd, 7.48; found, 7.99. ^d N: calcd, 13.15; found, 12.55. ^e Yield of **76** when 10 equiv of **8b** was used.

Table 2. [³H]Fnz Binding, TBPS Shift, Cl⁻ Current Changes, and Metrazole Antagonism Data for Imidazo[1,5-*a*]quinoxaline Piperazine Ureas with Varying A-Ring Substitution

compd	R ¹	R ³	R ^{6,7}	K _i (nM) ^a	[³⁵ S]TBPS shift ^{b,c}	ΔCl ⁻ current ^{b,c}		ΔCl ⁻ current ^{b,c}		metrazole ^d ED ₅₀ (95% confidence interval) mg/kg, ip
						α ₁ β ₂ γ ₂	5.0 μM/0.5 μM	α ₃ β ₂ γ ₂	5.0 μM	
39	H	H	H	4.11	0.04		/0.35			>50
40	Me	H	H	3.04	-0.018		0.0/0.50			>50
41	Me	Me	H	6.67	-0.82		-0.1/0.50			>50
42	Me	H	7-F	1.04	-0.14		0.0/0.50			35.3 (21.8-57.1)
43	Me	Me	7-F	2.69	0.44		-0.1/1.0			35.3 (21.8-57.1)
44	H	H	7-Cl	3.99	-0.02		0.0/0.40			>50
45	H	Me	7-Cl	10.87	0.57		0.98/	0.44		7.4
46	Me	H	7-Cl	3.27	0.48		0.3/0.85	0.54		3.7
47	Me	Me	7-Cl	4.48	-0.06		-0.2/1.0	1.00		14.8
48	Me	H	6-Cl	28.16	0.05		0.29/			>50
49	Me	Me	6-Cl	56.26	0.22		0.71/			>50
50	H	H	7-Me	14.7	0.30		0.40/0.55			21.0 (15.0-29.5)
51	Me	H	7-Me	4.66	0.38		0.30/0.84	0.1		
52	Me	Me	7-Me	9.50	0.11		1.37/	0.56		1.6
53	Me	H	6-Me	250	0.54		0.22/			>50
54	Me	Me	6-Me	470	0.48		0.33/			>50
55	Me	H	7-CF ₃	32.38	0.31		0.50/	0.1		21.0 (14.9-29.5)
56	Me	Me	7-CF ₃	31.42	0.26		0.81/			6.2
57^e	Me	H	7-Cl	19.93	1.23		0.96/	1.08		0.40
58^e	Me	Me	7-Cl	39.75	1.43		2.60/	0.68		0.60
diazepam				4.9	1.0 ± 0.2		1.0 ± 0.2	1.0 ± 0.2		0.50 (0.38-1.2)
1				1.0	0.69		0.68/			21
2				1.6	0.06		0.04			1.6

^a Mean binding affinity against [³H]flunitrazepam; see ref 28 and the Experimental Section for methods. The standard error was <±10% of the mean. ^b Diazepam is defined as a full agonist which gives a value of 1. Antagonists are defined as having a shift value of 0; partial agonists are intermediate. ^c See the Experimental Section. The standard error was <±10% of the mean. ^d Antagonism of metrazole-induced clonic convulsions in the rat after ip injection; see the Experimental Section. ^e *gem*-4,4-Dimethyl.

TBPS shift ratio, Cl⁻ current, and metrazole assays are provided in Tables 2-7.

Our initial screening efforts were directed toward the evaluation of the *cis*-3,5-dimethyl- and *cis*-3,5,4-trimethylpiperazine ureas with a variety of A-ring substituents. Most of these analogues had excellent affinity for the benzodiazepine receptor with K_i's typically between 1.0 and 15 nM as shown in Table 2. The major exceptions proved to be the 6-Cl (**49**) and 6-methyl (**54**) analogues with **54** having a K_i of 470 nM. The decreased affinity of the 6-substituted analogues is consistent with the SAR of the 3-phenyl analogues reported earlier¹⁵ and is in contrast to the typical benzodiazepine SAR.³⁸ Of the substituents examined at the 7-position, only the trifluoromethyl analogues (**55**, **56**) suffered a decrease in affinity (32 nM). Substitution on the A-ring was found to correlate quite well with intrinsic activity and potency in the metrazole antagonism assay. The unsubstituted analogues proved to be antagonists by TBPS shift and Cl⁻ current assays, with **41** a potent inverse agonist (TBPS shift = -0.82). Consistent with this potent inverse agonist activity, **41** did promote seizures at high doses (>100 mg/kg). This property is known for benzodiazepine inverse agonists.^{1,2} However, biphasic effects were observed in the Cl⁻ current screen with **39-41** behaving as partial agonists at 0.5 μM (Cl⁻ current 0.35-0.50). The 6-chloro and 6-methyl analogues were quite similar, with TBPS shift ratios and Cl⁻ current consistent with partial agonist intrinsic efficacy. None

of these analogues were active in the metrazole assay. The 7-fluoro analogues had greater efficacy with **43** being a full agonist at 0.5 μM in the chloride current screen. Both of these derivatives displayed biphasic properties and were weak metrazole antagonists. Substitution at the 7-position with a larger group (Cl, CH₃, CF₃) provided partial to full agonist analogues, many of which displayed potent metrazole antagonism activity. In the TBPS assay only **44** and **47** were antagonists, with the rest of the ureas partial agonists. Biphasic effects were clearly present with **47** displaying full agonist properties at 0.5 μM. This derivative, along with **45**, **46**, **52**, and **56**, was an effective metrazole antagonist. In comparing the simple piperazine ureas, an *N*-methyl group is important for activity, with **45** quite effective in the metrazole screen as compared to **44**. In contrast, the *N*-methyl group is not necessary for metrazole activity for the *cis*-3,5-dimethylpiperazine analogues. The requirement of a bulky 7-substituent for potent metrazole activity is unique to this *tert*-butyl ester series, as the corresponding 3-oxadiazole¹³ and 3-phenyl¹⁵ analogues were generally effective with unsubstituted A-rings. Substitution at the 4-position with *gem*-dimethyl groups was also tolerated, with **57** and **58** suffering only a 6-8-fold loss in binding affinity as compared to **46** and **47**. As with the corresponding 3-oxadiazole and 3-phenyl series, this substitution provided for enhanced efficacy, with **58** having a 2.6-fold greater Cl⁻ current than diazepam. Several ana-

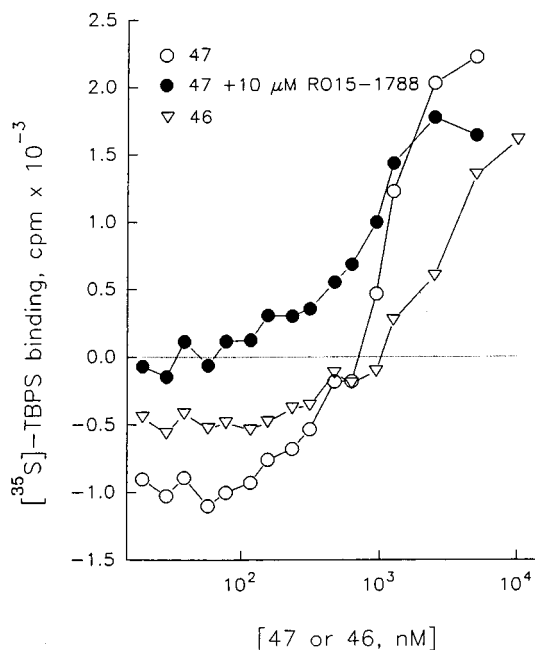


Figure 3. TBPS binding dose-response curve of **46** and **47**. Full agonist = -1.0 , antagonist = 0.0 , full inverse agonist = $+1.0$. Each point represents the average of three measurements with experimental errors less than 15%. Typically, diazepam at $1 \mu\text{M}$ reduced TBPS binding by $34 \pm 4\%$, while DCMC at $0.1 \mu\text{M}$ increased TBPS binding by 48%, under the same experimental conditions in this study.

logues within this subseries were evaluated for intrinsic efficacy in the $\alpha_3\beta_2\gamma_2$ subtype. Three analogues (**45**, **52**, **58**) had significantly less efficacy in the $\alpha_3\beta_2\gamma_2$ subtype as compared to $\alpha_1\beta_2\gamma_2$, while the rest of the derivatives evaluated showed no selectivity. Three analogues (**46**, **51**, **55**) were partial agonists in both subtypes.

The biphasic properties of several analogues within this series were explored in depth. The dose-response curves for **46** and **47** in the TBPS shift assay are shown in Figure 3. Both compounds at low concentrations reduced, and at high concentrations enhanced, [^{35}S]-TBPS binding. As previously reported for **47**,³⁹ the agonist properties of this compound are blocked by Ro 15-1788, an antagonist at the benzodiazepine site. The inverse agonist properties of **47** were not blocked by this BzD antagonist, indicating that this and other related quinoxaline piperazines also interact with a second site on the GABA_A receptor which is distinct from the benzodiazepine site. Analysis of the binding data for **47** in the presence of Ro 15-1788 indicates a single low-affinity site with an estimated K_d of 407 nM. Apparently, when **47** occupies this low-affinity site it allosterically influences the GABA_A receptor, leading to a reversal of agonist activity on the BzD site and inhibition of GABA-induced Cl^- current, effectively limiting its own agonistic actions. The bell-shaped dose-response profile of **47**, as monitored with GABA-induced Cl^- current, was also evident in the $\alpha_3\beta_2\gamma_2$ subtype as shown in Figure 4. In the $\alpha_6\beta_2\gamma_2$ subtype, **47** had no effect on Cl^- current at low concentration. However, at high concentrations in this subtype, the inverse agonist properties manifested by this compound at the low-affinity site were evident. Neither **46** nor **47** induced seizures at high doses ($>150 \text{ mg/kg}$).

To provide a comparison for the quinoxaline piperazines, a small number of simple urea analogues were

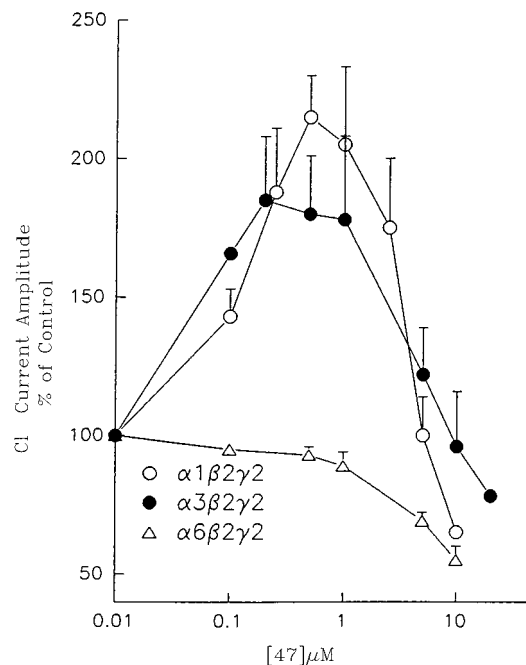
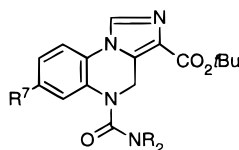


Figure 4. Cl^- current dose-response curve for **47** in several GABA_A receptor subtypes. Full agonist = 200, antagonist = 100, full inverse agonist = 0. Diazepam at $1 \mu\text{M}$ increased GABA currents by $143 \pm 44\%$ in the $\alpha_1\beta_2\gamma_2$ subtype and by $312 \pm 110\%$ in $\alpha_3\beta_2\gamma_2$.

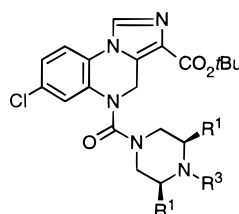
also evaluated with the results provided in Table 3. All of these analogues, regardless of the amine (NR_2) or R^7 substituents, had high binding affinity. The unsubstituted quinoxalines **59–61** ($\text{R}^7 = \text{H}$) were antagonists by the TBPS and Cl^- current assays, while the 7-chloro analogues had slightly enhanced intrinsic efficacy and were partial agonists. The TBPS shift ratio and Cl^- current values were nearly identical for each analogue with no biphasic effects observed. Only the 7-chloro analogues, **62** and **63**, were active in the metrazole screen, albeit to a moderate degree.

The SAR of the distal nitrogen substituent (R^3) was evaluated for both piperazine and *cis*-3,5-dimethylpiperazine moieties while maintaining a 7-chloro group on the A-ring. As shown in Table 4, the R^3 substituent had little effect on affinity with only **70** having a K_i of $>25 \text{ nM}$. Most analogues within this series were partial to full agonists based on the TBPS assay. The two exceptions, **64** (antagonist) and **69** (inverse agonist), contained bulky R^3 groups. Biphasic properties were evident for three analogues (**68–70**), with isopropyl-**69** displaying (like **47**) a particularly large change in chloride current between the different drug concentrations. Biphasic effects were absent for **71** and **72** which lack a basic nitrogen. Interestingly, **65–67** displayed enhanced Cl^- current with increased drug concentration, a property typically observed for BzR ligands. Clearly, the biphasic properties observed for compounds such as **47** and **69** are quite susceptible to modification of the R^3 substituent, in contrast to changes in the A-ring or 3-position where biphasic effects are maintained, indicating that the distal piperazine nitrogen may be involved with this unique property. Within this series only **65**, **68**, and **71** were effective metrazole antagonists. Interestingly, **67**, which was nearly a full agonist *in vitro*, was inactive in this assay. Of these

Table 3. [³H]Fnz Binding, TBPS Shift, Cl⁻ Current Changes, and Metrazole Antagonism Data for Imidazo[1,5-*a*]quinoxaline Piperazine Ureas with Varying A-Ring Substitution

compd	NR ₂	R ⁷	K _i (nM) ^a	[³⁵ S]TBPS shift ^{b,c}	ΔCl ⁻ current ^{b,c} α ₁ β ₂ γ ₂ 5.0 μM	metrazole ^d ED ₅₀ (95% confidence limits) mg/kg, ip
59	NMe ₂	H	5.25	0.15	0.09	> 50
60	piperidine	H	1.35	0.08	0.00	> 50
61	morpholine	H	2.47	0.00	0.14	> 50
62	NMe ₂	Cl	5.56	0.51	0.35	10.5 (5.2–21.4)
63	pyrrolidine	Cl	2.56	0.53	0.38	29.7

^a Mean binding affinity against [³H]flunitrazepam; see ref 28 and the Experimental Section for methods. The standard error was <±10% of the mean. ^b Diazepam is defined as a full agonist which gives a value of 1. Antagonists are defined as having a shift value of 0; partial agonists are intermediate. ^c See the Experimental Section. The standard error was <±10% of the mean. ^d Antagonism of metrazole-induced clonic convulsions in the rat after ip injection; see the Experimental Section.

Table 4. [³H]Fnz Binding, TBPS Shift, Cl⁻ Current Changes, and Metrazole Antagonism Data for Imidazo[1,5-*a*]quinoxaline Piperazine Ureas

compd	R ¹	R ³	K _i (nM) ^a	[³⁵ S]TBPS shift ^{b,c}	ΔCl ⁻ current ^{b,c} α ₁ β ₂ γ ₂ 5.0 μM/0.5 μM	metrazole ^d ED ₅₀ (95% confidence limits) mg/kg, ip
64	H	^t Bu	20.91	-0.03	0.12/	50
65	H	cPr	5.39	0.76	0.75/0.42	12.5 (6.0–26.0)
66	H	2-pyridyl	15.1	0.32	0.83/0.35	> 50
67	H	CH ₂ CF ₃	10.86	0.81	1.00/0.80	> 50
68	Me	Et	10.47	0.15	0.50/0.94	3.7 (2.6–5.2)
69	Me	ⁱ Pr	5.16	-0.97	-0.32/0.9	35.3 (21.9–57.1)
70	Me	CH ₂ CF ₃	37.84	0.67	0.00/0.5	42.0 (29.9–59.0)
71	Me	COCH ₃	4.66	0.94	0.79/	14.8
72	Me	SO ₂ Me	4.18	0.76	0.90/	> 50

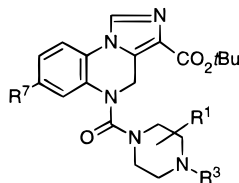
^a Mean binding affinity against [³H]flunitrazepam; see ref 28 and the Experimental Section for methods. The standard error was <±10% of the mean. ^b Diazepam is defined as a full agonist which gives a value of 1. Antagonists are defined as having a shift value of 0; partial agonists are intermediate. ^c See the Experimental Section. The standard error was <±10% of the mean. ^d Antagonism of metrazole-induced clonic convulsions in the rat after ip injection; see the Experimental Section.

analogues, only *N*-ethyl **68** was more effective than **45** in the metrazole assay.

As the *C*-methyl groups of **46** and related analogues have a profound effect on in vitro efficacy and metrazole antagonism as compared to unsubstituted **44**, a thorough SAR exploration of the regiochemistry of the appended methyl groups was undertaken. Reversal of the *cis*-dimethylpiperazine group provided reasonable affinity for the 7-fluoro analogues **73** and **74** (*K*_i's of 3.5 and 13 nM), while the 7-chloro analogue, **75**, had notably decreased binding affinity (Table 5). In vitro efficacy increased slightly for **73** and **74** as compared to the corresponding regioisomers (**42** and **43**), while the 7-chloro analogue, **75**, had significantly increased intrinsic efficacy as compared to **47**. The enhanced efficacy for this substitution pattern was also evident from the metrazole screening results, where all three analogues were quite potent. All of the other urea analogues, which had varying regiochemistry and number of *C*-methyl groups, had excellent affinity. The only exception proved to be **84** which, given the bulky bis-spirocyclohexylpiperazine, was reasonably well tolerated with a *K*_i of 79

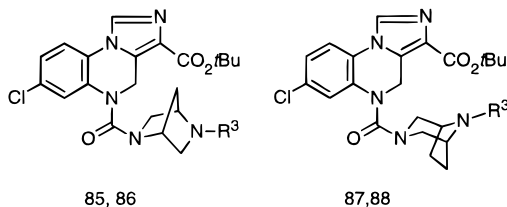
nM. In the TBPS shift assay, these analogues (**76**–**84**) ranged from partial inverse agonists (**78** and **84**) to nearly full agonists (**83**). Results from the Cl⁻ current screen reflected a similar efficacy range with biphasic properties observed for most analogues. Most of the *C*-methylpiperazine derivatives were effective in the metrazole screen, in contrast to unsubstituted **44**, with partial agonists **76**, **77**, and **79** particularly effective. The stereochemistry of the appended *C*-methyl groups often had significant effects on metrazole activity. In particular with the 2,3-dimethylpiperazine analogues, *cis*-analogue **79** was 25-fold more potent than the *trans*-regioisomer **80**, even though in vitro efficacy was nearly identical for the two analogues.

Two rigid bicyclic piperazine ring systems were evaluated (Table 6). All four analogues had reasonable binding affinity (5–30 nM) and were partial agonists as indicated by their TBPS shift ratios. Both *N*-methyl analogues had greater efficacy than diazepam in the chloride current screen, while the unsubstituted counterparts were partial agonists. Biphasic properties were noted for **86** and **87**, indicating that the additional cyclic

Table 5. [³H]Fnz Binding, TBPS Shift, Cl⁻ Current Changes, and Metrazole Antagonism Data for *C*-Methyl Imidazo[1,5-*a*]quinoxaline Ureas

compd	R ¹	R ³	R ⁷	K _i (nM) ^a	[³⁵ S]TBPS shift ^{b,c}	ΔCl ⁻ current ^{b,c} α ₁ β ₂ γ ₂ 5.0 μM/0.5 μM	ΔCl ⁻ current ^{b,c} α ₃ β ₂ γ ₂ 5.0 μM	metrazole ^d ED ₅₀ (95% confidence limits) mg/kg, ip
73	<i>cis</i> -2,6-di-Me	H	F	3.45	0.02	0.0/0.72		10.5 (5.1–21.3)
74	<i>cis</i> -2,6-di-Me	Me	F	13.3	0.63	0.75/		8.8 (5.4–14.3)
75	<i>cis</i> -2,6-di-Me	Me	Cl	90.2	1.02	1.71/	0.69	6.2
76	3-Me	H	Cl	4.48	0.18	0.17/0.5		8.8 (5.5–20.2)
77	<i>trans</i> -3,5-di-Me	H	Cl	2.35	0.41	0.8/0.60		10.5 (5.5–20.2)
78	<i>trans</i> -2,5-di-Me	H	Cl	7.80	-0.63	-0.05/0.3		17.6 (17.6–17.6)
79	<i>cis</i> -2,3-di-Me	H	Cl	2.34	0.27	0.0/0.70		0.70 (0.4–1.2)
80	<i>trans</i> -2,3-di-Me	H	Cl	4.03	0.07	0.48/0.68		17.7 (10.9–28.6)
81	3,3-di-Me	H	Cl	3.03	-0.01	0.0/0.33		>50
82	3,3-di-Me	Me	Cl	4.35	0.21	0.50/1.1		35.3 (21.8–57.10)
83	3,3,5,5-tetra-Me	H	Cl	3.20	0.77	1.14/		3.70 (2.2–6.3)
84	<i>bis</i> -spiro-cyclohexyl	H	Cl	79.47	-0.38	-0.70/0.1		>50

^a Mean binding affinity against [³H]flunitrazepam; see ref 28 and the Experimental Section for methods. The standard error was <±10% of the mean. ^b Diazepam is defined as a full agonist which gives a value of 1. Antagonists are defined as having a shift value of 0; partial agonists are intermediate. The standard error was <±10% of the mean. ^c See the Experimental Section. ^d Antagonism of metrazole-induced clonic convulsions in the rat after ip injection; see the Experimental Section.

Table 6. [³H]Fnz Binding, TBPS Shift, Cl⁻ Current Changes, and Metrazole Antagonism Data for Imidazo[1,5-*a*]quinoxaline Ureas

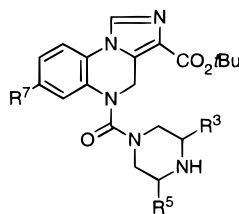
compd	R ³	K _i (nM) ^a	[³⁵ S]TBPS shift ^{b,c}	ΔCl ⁻ current ^{b,c} α ₁ β ₂ γ ₂ 5.0 μM/0.5 μM	metrazole ^d ED ₅₀ (95% confidence limits) mg/kg, ip
85	H	30.1	0.33	0.50/0.30	>50
86	CH ₃	4.89	0.68	1.0/1.6	7.4 (5.3–10.4)
87	H	5.45	0.20	0.2/0.73	>50
88	CH ₃	9.15	0.68	2.0/2.1	29.7 (17.7–49.9)

^a Mean binding affinity against [³H]flunitrazepam; see ref 28 and the Experimental Section for methods. The standard error was <±10% of the mean. ^b Diazepam is defined as a full agonist which gives a value of 1. Antagonists are defined as having a shift value of 0; partial agonists are intermediate. ^c See the Experimental Section. The standard error was <±10% of the mean. ^d Antagonism of metrazole-induced clonic convulsions in the rat after ip injection; see the Experimental Section.

structure and the boat conformation of piperazine **86** are tolerated. Only **86** was an effective metrazole antagonist.

Two piperazines from the *C*-methyl urea series (Table 5) were selected for further synthesis and pharmacological evaluation in chiral form. The targeting of the individual enantiomers of **76** and **77** was undertaken because of their partial agonist *in vitro* properties and anti-metrazole activity, as well as an interest to fully evaluate the SAR of the methyl groups at the 3- and 5-positions (as in **46**) of the piperazine ring system. The A-ring substituent was varied to include 7-Cl, 7-Me, and 7-CF₃, as several quinoxalines with these groups (i.e., **46**, **51**, and **55**) had excellent activity in the screening assays. As shown in Table 7, analogues from the 7-Cl and 7-Me series generally had good binding affinity (<25 nM) independent of the *C*-methyl stereochemistry. In contrast, the 7-CF₃ derivatives had decreased binding affinity, with **99** having a K_i of 277 nM. In the 3-methylpiperazine series, the 3-(*R*)-analogues had equal or

enhanced affinity over the (*S*)-enantiomers. Greater differences were noted for the *trans*-3,5-dimethylpiperazine ureas, with the (*R,R*)-analogues having 3–7-fold enhanced affinity over the (*S,S*)-antipodes. The TBPS shift ratios varied from antagonists to partial agonists, with most enantiomeric pairs having similar efficacy. The major exceptions proved to be the 7-methyl analogues where both the 3-(*S*)-Me and 3,5-(*S,S*)-dimethylpiperazines (**93** and **95**) had significantly enhanced intrinsic efficacy. Chloride current measurements for these chiral analogues varied from antagonists to full agonists. While most enantiomers had roughly equal efficacy, several exceptions were noted. The 3,5-(*S,S*)-dimethylpiperazine analogues in both the 7-Cl (**91**) and 7-CH₃ (**95**) series had 2-fold greater efficacy (at 0.5 μM) than their antipodes. Biphasic efficacy was also noted for most analogues. The major exceptions proved to be **95** and the 7-CF₃ analogues (**97**–**100**). These compounds lacked biphasic effects and were typically full agonists. Quinoxaline **91** had notably

Table 7. [³H]Fnz Binding, TBPS Shift, Cl⁻ Current Changes, and Metrazole Antagonism Data for Chiral Imidazo[1,5-*a*]quinoxaline Ureas

compd	R ³	R ⁵	R ⁷	K _i (nM) ^a	[³⁵ S]TBPS shift ^{b,c}	ΔCl ⁻ current ^{b,c} α ₁ β ₂ γ ₂ 5.0 μM/0.5 μM	metrazole ^d ED ₅₀ (95% confidence limits) mg/kg, ip
89	3(<i>S</i>)-Me	H	Cl	6.71	0.12	0.10/0.8	1.2 (0.9–4.0)
90	3(<i>R</i>)-Me	H	Cl	5.96	0.01	0.0/0.6	3.7 (2.1–6.7)
91	3(<i>S</i>)-Me	5(<i>S</i>)-Me	Cl	16.7	0.37	0.4/1.05	7.4 (3.5–15.9)
92	3(<i>R</i>)-Me	5(<i>R</i>)-Me	Cl	5.13	0.56	0.05/0.5	1.3 (0.6–2.8)
93	3(<i>S</i>)-Me	H	Me	17.9	0.59	0.4/1.1	25.0 (16.9–37.0)
94	3(<i>R</i>)-Me	H	Me	5.47	0.19	0.10/0.8	2.7 (1.4–5.1)
95	3(<i>S</i>)-Me	5(<i>S</i>)-Me	Me	25.6	0.77	1.3/1.3	7.4 (3.5–15.9)
96	3(<i>R</i>)-Me	5(<i>R</i>)-Me	Me	5.17	0.10	0.05/0.7	6.3 (3.0–13.1)
97	3(<i>S</i>)-Me	H	CF ₃	42.82	0.54	0.70/0.8	25.0
98	3(<i>R</i>)-Me	H	CF ₃	23.21	0.60	1.0/1.0	8.9 (3.9–20.4)
99	3(<i>S</i>)-Me	5(<i>S</i>)-Me	CF ₃	276.8	0.41	1.00/0.5	39.7 (8.4–186.3)
100	3(<i>R</i>)-Me	5(<i>R</i>)-Me	CF ₃	37.13	0.68	0.8/0.7	4.4 (2.7–7.2)

^a Mean binding affinity against [³H]flunitrazepam; see ref 28 and the Experimental Section for methods. The standard error was <±10% of the mean. ^b Diazepam is defined as a full agonist which gives a value of 1. Antagonists are defined as having a shift value of 0; partial agonists are intermediate. ^c See the Experimental Section. The standard error was <±10% of the mean. ^d Antagonism of metrazole-induced clonic convulsions in the rat after ip injection; see the Experimental Section.

decreased intrinsic activity in the α₃β₂γ₂ subtype (0.00) as compared to α₁β₂γ₂ (0.40). Most of the chiral piperazine ureas were effective metrazole antagonists with only the low-affinity analogues displaying correspondingly higher ED₅₀'s. Enantiomeric pairs often differed slightly in potency in this assay. However, this dissimilarity can be easily be rationalized by differences in binding affinity and intrinsic activity as detailed above.

On the basis of the results of the in vitro (binding, TBPS, chloride current) and metrazole assays, a number of the most promising compounds were evaluated further for in vivo efficacy, BzD antagonism, and typical benzodiazepine-type side effects (Table 8). Analogues were also evaluated in an ex vivo binding assay to determine CNS bioavailability and the duration of action after oral dosing. This ex vivo assay has been shown to be useful in evaluating these parameters for a number of BzD ligands.^{40a,b} In this screen, specific binding of the test drug, as determined through a (³H)-FNZ binding assay of brain homogenate after various periods of drug administration, is compared to the in vitro binding of the desired analogue. This ratio is directly related to the concentration of drug and its active metabolites in the brain. Within this series, the ex vivo assay proved to be predictive (with the caveat of including active metabolites) in identifying compounds with good oral activity.

The observed CNS availability of the piperazine ureas was superior to similar urea analogues (dimethylamino, piperidine, morpholine) which are lacking in a basic nitrogen. For instance, piperidine **60** had only 44% ex vivo binding as compared to 82% for **40**. In general, the *cis*-3,5-dimethylpiperazine substituent provided 70–95% ex vivo binding, with or without an *N*-methyl substituent. Interestingly, the 7-Cl, 7-F, and unsubstituted analogues had superior ex vivo binding as compared to those with 6-Cl, 7-Me, or 7-CF₃ groups.

Quinoxalines with *gem*-4,4-dimethyl substitution (**57**, **58**) or *N*⁴-substitution with a methyl, ethyl, or isopropyl group (**47**, **68**, **69**) also had excellent activity in the ex vivo assay. However, trifluoroethyl, acetyl, or sulfonyl substitution (**70**–**72**) in the dimethylpiperazine series led to dramatically decreased apparent oral bioavailability. Reversal of the *cis*-dimethylpiperazine (**73**–**75**) resulted in rapid clearance from the CNS, although **73** and **74** had acceptable ex vivo binding. All of the simple piperazines (R¹ = R² = H) containing various NR³ substituents had poor ex vivo activity (or were cleared rapidly) further highlighting the unique properties of the 3,5-methylated piperazine group. Of the *C*-methylpiperazine regioisomers evaluated, the 3-methyl- (**76**), *trans*-3,5-dimethyl- (**77**), and 2,3-dimethylpiperazine isomers (**79**, **80**) had reasonable ex vivo binding with a long duration of action. Like the *cis*-2,6-dimethylpiperazines, the *gem*-3,3-dimethylpiperazines **81**–**83** were cleared rapidly. None of the bicyclic analogues were particularly effective in this assay. Evaluation of the chiral 3-methyl and *trans*-3,5-dimethyl analogues in the ex vivo assay resulted in a similar SAR to that observed for **46** and related analogues. In particular, the 7-chloro analogues had excellent CNS bioavailability while the 7-CH₃ and 7-CF₃ analogues were notably inferior.

Analogues having reasonable oral activity and duration of action in the ex vivo screen were also evaluated in a stress-induced cyclic 3',5'-guanosine monophosphate (cGMP) assay. Acute stress by electroconvulsive shock, electric footshock, immobilization, or forced swimming in ice-cold water has been shown to increase cGMP levels.^{41,42} Numerous BzD anxiolytic agents are effective in lowering the levels of cGMP after electric footshock stress.^{41b,42} This biochemical model of stress has proven to be sensitive and useful in predicting anti-stress and anxiolytic activity of many standard anxiolytic agents. For example, diazepam and **2** were both potent, lowering the cGMP to control levels (80/182 and

Table 8. Benzodiazepine Antagonism, ex Vivo Binding, cGMP, and Acute Physical Dependence Data for Imidazo[1,5-a]quinoxalines

compd	acute electroshock physical dependence activity ^a (drug MA ₅₀ /V122 MA ₅₀)	oral ex vivo binding assay ^b max % inhibition (time in min for peak effect)	cerebellar GMP assay ^c % control ((drug + stress)/stress)	BZD antagonism ^d ED ₅₀ (95% confidence interval) mg/kg
40		82 (60)	148/157	>30
42		95 (60)	126/171	>30
43		94 (60)	131/171	21.8 (10.6–44.8)
45	A (14.4/20.5)	29 (30)	152/162	11 (5.0–22.0)
46	A (18.0/21.3)	71 (240)	131/205	>30
47	IA (18.1/17.7)	86 (120)	70/195	7.0 (3.0–18.0)
48		44 (30) ^e	162/171	>30
49	IA (18.1/19.2)	49 (60)	176/171	>30
50	A (18.2/25.8)			>30
51	A (16.5/19.7)	55 (240)	115/157	>30
52	A (15.9/21.3)	64 (30)	93/162	>30
55	IA (19.2/19.2)	52 (120)	73/205	>30
56	A (17.3/21.0)	17 (240)		21.8 (10.6–44.8)
57	A (13.9/18.8)	94 (60)	63/206	
58	A (11.5/17.7)	84 (30)	79/206	>30
60	IA (19.2/21.2)	44 (60)	178/195	4 (2–9)
63	IA (20.8/21.2)		174/166	14 (7–28)
64	A (20.9/24.0)	62 (30)		>30
65	IA (21.9/23.8)	24 (240)		>30
66	A (17.9/24.0)	3.4 (120)		>30
67	IA (25.2/25.2)	10 (240)		>30
68	IA (19.2/19.9)	84 (30)	180/205	>30
69	IA (19.2/18.4)	85 (30)	114/220	>30
70	IA (24.9/23.8)	19 (240)		>30
71	A (18.9/21.9)	22 (60)		>30
72	IA (18.9/19.7)	8 (120)		>30
73		69 (30) ^e	173/171	>30
74		68 (30) ^e	141/171	>30
75	IA (18.5/17.7)	32 (30) ^e	204/205	>30
76	A (15.6/23.8)	68 (240)		>30
77		63 (60)		17.3 (7.9–37.9)
78	A (17.7/19.7)	71 (60)		>30
79	A (15.4/18.4)	78 (60)	154/220	>30
80	A (21.9/25.8)	55 (30)		35 (19.4–61.6)
81	IA (24.0/24.9)	13 (30) ^e		>30
82	IA (25.6/23.8)	11 (30) ^e		>30
83	A (25.8/27.7)	47 (30) ^e	67/165	>30
85	IA (21.6/24.0)	4 (60)		>30
86		11 (60)		>30
88	A (18.5/24.9)	26 (30)		>30
89	A (19.4/25.6)	74 (30)	100/177	>30
90	A (16.1/23.6)	75 (30)	104/177	27.5 (15.4–48.9)
91	IA (24.6/25.2)	45 (60)	124/179	>30
92	A (19.2/25.2)	62 (120)		>30
93	A (19.9/26.9)	32 (60)	102/183	>30
94	A (20.7/23.5)	51 (240)	108/183	17.3 (7.9–37.9)
95	A (20.7/24.0)	17 (120)	152/193	>30
96		22 (30)	86/173	
97	IA (23.0/23.6)	21 (120)	162/198	>30
98	A (17.9/26.9)	30 (240)	159/180	>30
99	A (22.6/26.9)			>30
100		24 (30)	167/180	>30
diazepam	A ^f (18.2/25.4)		80/182	>30
1	IA (23.2/24.9)		119/195	1.0
2	IA (21.2/22.2)		137/158	1.7 (0.8–3.8)

^a A, $p < 0.05$; IA, no significant activity; see the Experimental Section. ^b See the Experimental Section. The standard error was $< \pm 5\%$ of the mean. ^c See the Experimental Section. The standard error was $< \pm 10\%$ of the mean. ^d See the Experimental Section. ^e Low levels ($< 10\%$) of the test compound detected at 60 min. ^f Tested at 15 mg/kg.

119/195 of (drug + stress)/stress response, respectively). In this assay, the levels of cGMP (baseline = 100%) were measured in mice receiving drug after electric foot shock stress. These levels were compared to a control group which received vehicle prior to the shock treatment. The resultant values are expressed as percent of control for (drug + stress)/stress animals, respectively.

A significant number of the quinoxaline piperazines were effective in lowering cGMP levels after applied stress. This is in sharp contrast to the piperidine and pyrrolidine analogues (**60** and **63**, respectively) which were inactive. Within the *cis*-3,5-dimethylpiperazine

series, a bulky substituent at the 7-position of the A-ring (Cl, Me, CF₃) was required, with **46** and **55** particularly effective. The unsubstituted and 6-chloro analogues were inactive, while the 7-fluoro quinoxalines were weakly active, paralleling their limited anti-metrazole activity. An *N*-alkyl substituent was also tolerated in this ring system, with **47**, **52**, and **69** having excellent anti-stress activity, although the *N*-ethyl derivative **68** was inactive. The two *gem*-4,4-dimethyl full agonist analogues (**57** and **58**) were also extremely effective. Both the *cis*-2,6-dimethylpiperazines and the only simple piperazine tested, **45** (which lacked a *C*-methyl group),

were ineffective. Regioisomeric methyl groups were also tolerated on the piperazine ring with *cis*-2,3-dimethylpiperazine (**79**) and 3,3,5,5-tetramethylpiperazine (**83**) analogues effective. In the chiral piperazine series, all analogues tested with a 7-Cl or 7-Me group were active (except **95**), whereas the 7-CF₃ derivatives were ineffective. This latter result was quite surprising given the potent anti-stress properties of **55**. A good correlation between anti-stress activity in the cGMP assay to metrazole antagonism properties and ex vivo binding was noted for most analogues. In particular, those compounds which were potent in the metrazole assay and which also had reasonable CNS availability by ex vivo assay were generally effective in the cGMP screen. Exceptions were **69**, which was a weak metrazole antagonist yet was potent in the cGMP assay, and the 7-methyl analogues (**93–96**), which typically performed poorly by ex vivo assay but were effective in the cGMP screen. Consistent with the above, compounds which had weak metrazole activity or poor ex vivo binding were typically ineffective in the cGMP assay. Several apparent exceptions (**68**, **73–75**) most likely result from rapid clearance from the CNS (as determined by the ex vivo assay).

Most of the compounds were also evaluated for their ability to antagonize the muscle relaxation effects of a benzodiazepine full agonist, triazolam. Traction was assessed 30 min after separate administration of triazolam and the test compound. The antagonist flumazenil, at 2.0 mg/kg, was effective in blocking the muscle-relaxing effects of triazolam, as were partial agonists **1** (1.0 mg/kg) and **2** (1.7 mg/kg). Traditional full agonist benzodiazepine ligands are not effective in blocking muscle relaxation in this assay. In general, the quinoxaline piperazines were not benzodiazepine antagonists, with only **45** and **47** having reasonably low ED₅₀'s (11.0 and 7.0 mg/kg, respectively). The two nonpiperazine analogues (**60**, **63**) evaluated were also BzD antagonists. Derivatives from this series, like those reported in the 3-phenyl classes,¹⁵ display little correlation between intrinsic efficacy and BzD antagonism. This discrepancy apparently is not due to poor CNS penetration or extensive metabolism to inactive metabolites, as many analogues displayed excellent activity by ex vivo assay.

Physical dependence is one of the more undesirable side effects typically promoted by benzodiazepine full agonists. Clinically, manifestations of physical dependence are undesirable, as they are similar to the disorder being treated.⁴³ The degree of acute physical dependence was assessed through an electroshock seizure assay.⁴³ Withdrawal from chronic treatment with high doses of benzodiazepines may in some cases result in signs and symptoms related to hyperexcitability of the CNS. In animals, such changes can be quantified by determining the current threshold (MA₅₀) to elicit electroshock-induced seizures. The lowering of the electroshock threshold precipitated by a benzodiazepine antagonist after an acute regimen of test compound was used to quantify the development of physical dependence. Mice received the test drug for 3 days (150 mg/kg/day). Twenty-four h after the last administration, the mice received an iv injection of a benzodiazepine antagonist (flumazenil). Five minutes later, the mice were

Table 9. Vogel's Punished Licking Assay

compd	dose (mg/kg)	<i>n</i>	mean no. of shocks ^a
46	0	9	3.8 ± 0.3
	0.3	10	5.3 ± 0.8
	1.0	10	3.1 ± 0.3
	3.0	10	5.7 ± 0.8
	10.0	10	12 ± 2.6**
	12 mg/kg CDPZ	10	19 ± 4.1**
47	0	10	8.4 ± 3
	0.3	10	8 ± 2
	1.0	10	7 ± 3
	3.0	9	18 ± 4*
	10.0	6	18 ± 5
	3 mg/kg diazepam	10	13 ± 3
55	0	8	4.9 ± 1.2
	0.3	8	4.6 ± 0.9
	1.0	8	4.9 ± 0.8
	3.0	9	6.4 ± 0.9
	10.0	9	7.9 ± 1.2*
	12 mg/kg CDPZ	9	23 ± 4**
69	0	8	6.6 ± 0.7
	0.3	9	6.3 ± 1.8
	1.0	10	5.3 ± 0.6
	3.0	9	5 ± 1
	10.0	9	3.4 ± 0.4**
	12 mg/kg CDPZ	8	26 ± 4.8
91	0	9	3.3 ± 0.4
	0.3	10	3.9 ± 1
	1.0	10	5.2 ± 1.2
	3.0	10	5.6 ± 1.2
	10.0	10	8.8 ± 2**
	12 mg/kg CDPZ	10	14.8 ± 3.9**

^a Single asterisk (*) indicates $p < 0.05$ and double asterisk (**) $p < 0.01$ compared to "0" group in that experiment using Wilcoxon rank sum test.

assessed for electroshock seizure thresholds (MA₅₀ compared to vehicle MA₅₀), which typically were lower for mice undergoing flumazenil-precipitated withdrawal. Standard benzodiazepine ligands such as diazepam were active in this paradigm at doses as low as 15 mg/kg/day, while partial agonists **1** and **2** were not.

Many of the compounds evaluated in the acute electroshock physical dependence assay were active, regardless of their in vitro efficacy. Quinoxalines **57** and **58** were particularly active. The two nonpiperazine analogues (**60**, **63**) were inactive. Not surprisingly, analogues which had poor ex vivo binding properties were usually inactive, although exceptions such as **66** were noted. Nonetheless, the correlation was quite good, especially considering the different dosing regimes. Importantly, several compounds (**47**, **55**, **69**, **91**) were identified which had reasonable properties in the metrazole, cGMP, and ex vivo assays, yet lacked physical dependence. Another extremely interesting result from the physical dependence assay was the enantiomeric pair **91** and **92**. While **91** had slightly decreased affinity and ex vivo binding as compared to its enantiomer (**92**), the lack of physical dependence for this analogue is quite surprising and indicates that minor structural changes can have an impact on overt side effects.

On the basis of their efficacy and side effect profile, several analogues (**47**, **55**, **69**, and **91**) were selected for evaluation in Vogel's punished licking assay.^{9a} Even though it produced a moderate degree of physical dependence, **46** was included due to its close relationship to some of the lead compounds. As shown in Table 9, **47** was the most effective compound, significantly active at 3 mg/kg (and nearly so at 10 mg/kg). In this

Table 10. Geller–Cook Activity of **46** and **47**

treatment	dose (mg/kg)	<i>n</i>	punished rate ^a	nonpunished rate ^a
control	0	12	23 ± 2	35 ± 2
46	1.0	6	46 ± 16*	47 ± 12
46	3.0	6	27 ± 9	43 ± 11
control	0	17	18 ± 4	34 ± 4
47	0.3	6	22 ± 12	38 ± 5
47	1.0	6	53 ± 20*	56 ± 19
47	3.0	6	65 ± 16*	36 ± 6

^a Asterisk (*) indicates $p < 0.05$ compared to own control using Wilcoxon signed rank test.

particular screen **47** was more effective than 3.0 mg/kg of diazepam. Three of the other analogues (**46**, **55**, **91**) were also active (10 mg/kg), although they were less effective than 12 mg/kg of chlordiazepoxide. Interestingly, **69** significantly decreased the number of shocks taken at 10 mg/kg (inactive at lower doses), possibly consistent with its potent inverse agonist properties noted at 5 μ M in the chloride current assay. Two of these analogues (**46**, **47**) were also evaluated in the Geller–Cook conflict assay,^{9a} with data provided in Table 10. As shown, both of these quinoxalines were active on punished schedule components at 1 mg/kg with **47** also effective at 3 mg/kg. Consistent with their partial agonist profile, neither analogue was active on nonpunished components.

The pharmacokinetics and oral bioavailability of the four compounds active in the Vogel assay were evaluated in rats, with data shown in Table 11. Among these compounds, **47** had the highest total plasma clearance (2.71 L/h/kg) and the shortest terminal elimination half-life, averaging 0.57 h after iv administration. Serum concentrations of **47** in rats after oral administration were all below the limit of quantitation. A major metabolite with much higher serum concentration than the parent was observed after oral administration of **47** to rats and was identified as the N-demethylated product of **47**, namely **46**. These data suggest that **47** is subject to metabolic clearance and is not orally bioavailable due to extensive first-pass metabolism in rats. Quinoxaline **46** was much more metabolically stable in rats, with a 2-fold lower total plasma clearance and 2-fold longer half-life as compared to **47**. The oral bioavailability of **46** in rats was nearly 100%, showing limited first-pass metabolism of this compound after oral dosing. The trans isomer of **46** (**91**) had lower plasma clearance and a longer half-life in rats than **46**. However, the oral bioavailability of **91** was only 54%, suggesting a more significant first-pass effect of **91** after oral administration. Quinoxaline **55**, with a 7-trifluoromethyl substituent replacing the chloro of **46**, had the lowest plasma clearance (0.73 L/h/kg) and longest half-life (2.4 h) in rats. The oral bioavailability of **55** averaged 84%. These data suggest that the trifluoromethyl replacement further improved the in vivo metabolic stability. The evaluation of the pharmacokinetics of pyrrolidine urea **63** was also undertaken (po dosing only) to provide a comparison to the piperazine analogues. As indicated in the table, this analogue had a significantly lower C_{\max} (0.33 mg/mL) as compared to **46** (1.17 mg/mL), although it had a longer $t_{1/2}$ (7.6 h). A major metabolite was observed for **63**. The concentration ratio (metabolite/parent) was approximately 0.5, indicating significant first-pass metabolism for **63**. This

first-pass metabolism was minimized through the 3,5-dimethylpiperazine substitution.

Molecular Conformations. The low-energy conformers of a number of compounds were determined by molecular mechanics methods. Calculations were performed using both the AMBER* and MM2* force fields, which were developed for the MacroModel⁴⁴ system of programs as extensions of the original AMBER⁴⁵ and MM2⁴⁶ parameter sets. Initial structures to be minimized were generated by means of an internal coordinate Monte Carlo procedure⁴⁷ in which torsional angles around all rotatable bonds were allowed to vary. In a typical calculation, 100–200 initial structures were minimized, and duplicate minimized structures were eliminated to give a final set of conformers. Energy-minimized structures were also obtained from semi-empirical quantum mechanical calculations using the MOPAC program⁴⁸ with the AM1⁴⁹ parameter set. The latter method was applied selectively, using the four or five lowest-energy conformers obtained from the molecular mechanics studies as initial structures.

Figure 5 shows face and edge views of two low-energy structures for **46**, obtained with the MM2* force field. Structures A and B are identical except for the orientations of the 5-substituent, which differ by a 180° rotation about the N₅–C bond. Both structures contain a planar region composed of the imidazoquinoxaline ring and 3-carboxylate moiety, with the *tert*-butyl and piperazine functional groups occupying different out-of-plane regions. Calculations using both the AMBER* force field and the MOPAC/AM1 method yielded structures with no significant geometrical differences from those obtained with MM2*. It should be noted that for each structure shown there exists a pair of mirror image isomers of identical energy which differ geometrically due to different puckering of the imidazoquinoxaline ring.

In both the present and previous computational studies of imidazoquinoxaline ureas,^{13,15} the identity of the lowest-energy conformer could not be unequivocally determined. In the case of **46**, MM2*-based calculations predicted structure A to be most stable, with structure B higher in energy by 3.25 kcal/mol. Moreover, three other conformers not shown in Figure 5 were found with energies between those of structures A and B. Specifically, structures differing from A by (a) a 180° rotation of the ester group about the C₃–C bond, (b) a 180° rotation of the carbonyl-*N*-piperazine bond (N1'–CO), and (c) rotations a and b combined were obtained with respective energies 0.37, 2.16, and 2.51 kcal/mol higher than that of structure A.

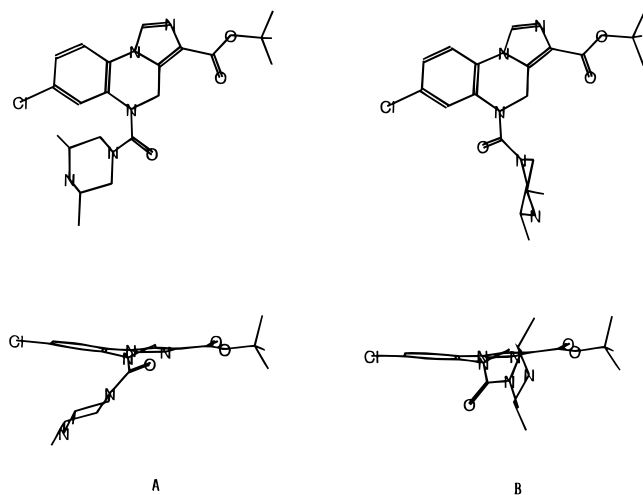
In contrast, both the AMBER*- and AM1-based calculations predicted structure B to be more stable than A by 0.93 and 2.09 kcal/mol, respectively. Furthermore, according to the AMBER*-based studies, a 180° rotation of the ester group as in rotation "a" above did not result in any energy increase, while the piperazine rotamer equivalent to rotation "b" above was higher in energy relative to structure B by approximately 0.84 kcal/mol.

The structures and relative energies of the majority of the other piperazine imidazoquinoxaline ureas were expected to be very similar to those described above for **46**. This was found to be the case in selected studies on **39**, **47**, and piperidine analogue **60**. With the 6-methyl

Table 11. Selected Pharmacokinetic Parameters following Intravenous (iv) and Oral (po) Administration of **46**, **47**, **55**, **63**, or **91** in a Solution Formulation to the Male Sprague–Dawley Rats

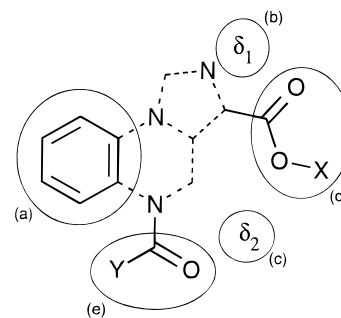
compd	route	n	dose (mg/kg)	C _{max} (μg/mL)	t _{max} ^a (h)	AUC (μg·h/mL)	t _{1/2} (h)	Cl _p (L/h/kg)	F ^b (%)
46	iv	4	5.10 ± 0.21	1.17 ± 0.49	0.5–4	3.54 ± 0.81	1.2 ± 0.3	1.51 ± 0.39	101
	po	4	5.22 ± 0.15			3.57 ± 0.99	1.8 ± 0.3		
47	iv	3	4.74 ± 0.29	c	c	3.46 ± 3.30	0.57 ± 0.22	2.71 ± 1.85	c
	po	3	4.75 ± 0.05			c	c		
55	iv	4	4.97 ± 0.03	1.16 ± 0.83	1–2	7.47 ± 2.72	2.4 ± 0.3	0.73 ± 0.28	84
	po	4	5.03 ± 0.07			6.43 ± 5.34	2.7 ± 0.6		
63	po	3	5.46 ± 0.09	0.33 ± 0.07	1–2	3.68 ± 0.54	7.6 ± 1.4	1.07 ± 0.32	54
	iv	4	5.06 ± 0.06			5.01 ± 1.21	1.5 ± 0.2		
91	iv	4	5.06 ± 0.06	0.66 ± 0.14	0.25–0.5	2.62 ± 1.08	2.4 ± 0.7		
	po	4	5.01 ± 0.11			2.62 ± 1.08	2.4 ± 0.7		

^a Data presented are the value range. ^b Calculated using average AUC. ^c Compound **47** serum concentrations below the lower limit of quantitation (50 ng/mL).

**Figure 5.** Molecular structures of relevant low-energy conformers of **46**. Hydrogen atoms are not shown.

analogue, **53**, calculated structures and energetics were also similar to those described for **46** although the piperazine substituent in **53** was positioned somewhat more out-of-plane than that in **46**, due to increased puckering in the imidazoquinoxaline ring. For the *gem*-dimethyl analogue, **57**, the calculated structures remained similar to those of **46**. However, in contrast to **46**, all three computational methods predicted structure A to be more stable than structure B, with energy differences of 6.67, 3.35, and 0.77 kcal/mol from the MM2^{*}, AMBER^{*}, and AM1-based calculations, respectively. This preference of structure A over B has been found in other *gem*-dimethyl imidazoquinoxalines as well.¹³

Pharmacophore Models. As discussed in previous publications,^{13,15} the imidazoquinoxaline series of benzodiazepine receptor ligands (BzR) has been shown to possess a number of features consistent with general models of BzR recognition and activation given by Wermuth et al.⁵⁰ and Gardner.^{4a} These models hold for the present analogues as well. Referring to Figure 6, the fused phenyl ring and divalent nitrogen (N₂) of the imidazoquinoxaline ring system correspond, respectively, to the aromatic group and hydrogen-acceptor site δ₁, considered to be essential for receptor recognition. A second H-acceptor site δ₂ may correspond to the R⁵ carbonyl group, provided that it is oriented as in structure A in Figure 5. In the Wermuth model, the distance between δ₁ and δ₂ was given as 3.2 Å. However, in an alternative model, Cook⁵¹ has suggested that this distance be extended to as large as 6.5 Å, a value consistent with the present structures.

**Figure 6.** Elements of the Wermuth and Gardner pharmacophoric models: (a) aromatic region, (b) and (c) hydrogen-acceptor site points δ₁ and δ₂, (d) freely rotating substituent, and (e) out-of-plane substituent.

Region d has been characterized as containing a “freely-rotating aromatic group” by Wermuth⁵⁰ or an ester group according to Gardner,^{4a} and the present *tert*-butyl ester corresponds to the latter case. In previous studies of 3-phenyl imidazoquinoxaline analogues,¹⁵ it was shown that BzR binding affinity could be substantially reduced by forcing the 3-phenyl substituent into an out-of-plane orientation relative to the imidazoquinoxaline ring. In the present analogues, the 3-carboxylate group was found to be in-plane in all of the calculated structures, which is consistent with the high affinity generally observed. However, the receptor will tolerate some out-of-plane character in this region, as exemplified by the *tert*-butyl group shown in Figure 5.

As described above in detail for **46**, the piperazine urea substituent in the present analogues is predicted to assume a number of possible orientations, all of which may be characterized as out-of-plane. An out-of-plane substituent in region e of Figure 6 has been associated with full agonist activity according to Wermuth et al.,⁵⁰ which may explain how minor changes with the piperazine substituent can dramatically modulate efficacy. The aryl substituents, R⁶ or R⁷, which have only a minimal effect on the urea conformation, presumably modulate efficacy through electronic effects. In summary, the quinoxaline piperazine ureas described herein are consistent with a model in which an aromatic region and one or perhaps two hydrogen-acceptor sites allow for receptor recognition (affinity), while efficacy is largely controlled by the cooperative effects of the aromatic R⁶ or R⁷ substituent and the out-of-plane R⁵ urea.

Conclusion

Compounds within the imidazo[1,5-*a*]quinoxaline piperazine series are high-affinity ligands for the GABA_A/

benzodiazepine receptor. Through manipulation of the substituents at the 5-, 6-, and 7-positions, analogues of widely varying intrinsic efficacy were identified. Typically, the combination of a 3,5-dimethylpiperazine urea with a bulky 7-substituent provided analogues with partial agonist *in vitro* activity. Furthermore, this substitution pattern generally resulted in excellent activity in a number of *in vivo* models measuring anxiolytic and anticonvulsant activity, including the metrazole and cGMP assays. Additionally, several analogues (**46**, **47**, **55**, **91**) were also found to be active in the Vogel punished licking assay. Most derivatives from this series were evaluated in an electroshock physical dependence screen with a number of the quinoxalines identified which did not produce this undesired BzD side effect. The degree of CNS penetration, as well as the duration of action in brain, was determined for a number of these derivatives by *ex vivo* assay, with the *cis*-3,5-dimethylpiperazine ureas typically providing for superior activity. Pharmacokinetic evaluation of five of the more interesting quinoxalines confirmed the results of the *ex vivo* assay, with **46** and **55** having 100% and 84% bioavailability, respectively. From the combination of these assays, **55** and **91** were identified as partial agonists which were effective in models of anxiety, had excellent pharmacokinetics, and yet were consistent with the partial agonist hypothesis by producing no major BzD side effects.

The biphasic nature expressed by many of the quinoxaline piperazine ureas, as determined by *in vitro* analysis, sets this series apart from other BzD ligands. The dual functionality observed for **46**, **47**, and **91** is, to our knowledge, unprecedented among BzD ligands. Therapeutically, compounds within this class could be unique due to their ability to limit their own agonistic actions. This property should effectively control the agonistic activity of these and related piperazine ureas over a wide range of doses and may serve to limit their abuse potential. Further pharmacological evaluation of selected analogues from this series will be reported in due course.

Experimental Section

Chemistry. Thin-layer and flash chromatography utilized E. Merck silica gel (230–400 mesh). Melting points were taken on a Thomas-Hoover capillary melting point apparatus and are uncorrected. Mass spectra, infrared spectra, and combustion analysis were obtained by the Physical and Analytical Chemistry Department of the Upjohn Co. ¹H NMR spectra were recorded at 300 MHz with a Bruker Model AM-300 spectrometer.

In cases where synthetic intermediates or products were isolated by "aqueous workup (organic solvent, drying agent)", the procedure was to quench the reaction with H₂O, dilute with the indicated organic solvent, separate the organic layer, extract the aqueous layer several times with the organic solvent, dry the combined organic layers with the indicated drying agent, filter off the drying agent, and remove the solvent using a rotary evaporator at reduced pressure. When "basic workup (organic solvent, aqueous basic solvent, drying agent)" is indicated, the procedure was similar to aqueous workup, except the indicated aqueous base was used instead of H₂O. When "acidic workup (organic solvent, organic solvent, drying agent)" is indicated, the procedure was to dilute the reaction mixture with the first indicated solvent, extract the organic solution several times with 10% HCl, basify the combined acidic layers with solid KOH, extract the basic solution with the second indicated organic solvent several

times, dry the organic layers with the indicated drying agent, filter off the drying agent, and remove the solvent using a rotary evaporator under reduced pressure. Tetrahydrofuran (THF) and ether were distilled from sodium and benzophenone. Dichloromethane was distilled from calcium hydride, and DMF was dried over 3 Å molecular sieves. All other solvents were EM Science HPLC grade, distilled in glass. Diethyl chlorophosphate and potassium *tert*-butoxide (1.0 M in THF) were purchased from the Aldrich Chemical Co., Milwaukee, WI. Phosgene in toluene (**CAUTION:** phosgene is highly toxic and should be used with extreme care) was purchased from Fluka Chemie AG or Columbia. All reactions were run under nitrogen or argon.

7-Chloro-4,5-dihydroimidazo[1,5-*a*]quinoxaline-3-carboxylic Acid 1,1-Dimethylethyl Ester (6c**).** Potassium *tert*-butoxide (60.0 mL, 60.0 mmol, 1.0 M in THF) was added to a solution of 6-chloro-1,2,3,4-tetrahydroquinoxalin-2-one¹³ (**5c**; 10.0 g, 54.8 mmol) and THF (180 mL) at –20 °C. The solution was allowed to warm to 0 °C over 30 min and was cooled to –40 °C. Diethyl chlorophosphate (9.00 mL, 62.3 mmol) was added and the solution allowed to warm to room temperature over 30 min. The solution was cooled to –78 °C, and a solution of the *tert*-butyl isocyanacetate (9.00 g, 63.8 mmol) and THF (15.0 mL) was added. Potassium *tert*-butoxide (60.0 mL, 60.0 mmol) was then added dropwise over several minutes. The solution was stirred at –78 °C for 30 min and then allowed to warm to room temperature over 2 h. After stirring at room temperature for 3 h, aqueous workup (ethyl acetate, MgSO₄), concentration, and trituration of the residue with hexane/ethyl acetate gave 9.42 g of **6c** as a mauve powder. Purification of the filtrate by flash chromatography (1:1 ethyl acetate:hexane) and trituration (ether/hexane) gave an additional 1.27 g (10.7 g total, 64%) of product (mp 261–263 °C): IR (mineral oil) 1683, 1522, 1367, 1323, 1302, 1254, 1154, 1057, 968 cm⁻¹; ¹H NMR (300 MHz, CDCl₃) δ 7.93 (s, ArH), 7.30 (d, *J* = 8.4 Hz, ArH), 6.75–6.85 (m, ArH), 6.79 (s, ArH), 4.81 (s, NCH₂), 4.13 (br s, NH), 1.61 (s, 'Bu); MS (EI) *m/e* 305, 249, 231, 203.

Example Procedure for the Synthesis of Urea 10 from Amine 6. Method A: 7-Chloro-5-[(1-(*cis*-3,5-dimethyl)piperazino)carbonyl]-4,5-dihydroimidazo[1,5-*a*]quinoxaline-3-carboxylic Acid 1,1-Dimethylethyl Ester (46**).** Triphosgene (643 mg, 2.17 mmol) was added to a mixture of **6c** (1.20 g, 3.92 mmol), CH₂Cl₂ (42 mL), and diisopropylethylamine (0.80 mL, 4.6 mmol) at 0 °C. The mixture was stirred for 1 h at 0 °C and then allowed to warm to room temperature. After stirring for 3 h, the resultant solution was cooled to 0 °C. Diisopropylethylamine (0.80 mL, 4.6 mmol) and *cis*-2,6-dimethylpiperazine (766 mg, 6.71 mmol) were added successively. The solution was stirred at 0 °C for 1 h and at room temperature for 16 h. Basic workup (CH₂Cl₂, NaHCO₃, MgSO₄) and purification by flash chromatography (5:1 ethyl acetate:MeOH) gave 1.59 g of the urea as a foam. Crystallization from ether/hexane provided 1.39 g (80%) of **46** as a tan powder (mp 200.5–201 °C): IR (mineral oil) 1689, 1643, 1512, 1424, 1316, 1306, 1159, 1154, 967 cm⁻¹; ¹H NMR (300 MHz, CDCl₃) δ 7.99 (s, ArH), 7.45 (d, *J* = 8.6 Hz, ArH), 7.10–7.20 (m, ArH, 2 H), 4.94 (s, ArNCH₂), 3.67 (d, *J* = 13.8 Hz, 2 H), 2.80–2.95 (m, 2 H), 2.48 (apparent t, *J* = 11.5 Hz, 2 H), 1.63 (s, 'Bu), 1.03 (d, *J* = 6.3 Hz, CHCH₃, 6 H); MS (EI) *m/e* 445, 389, 318, 306, 276, 248, 230, 141. Anal. (C₂₂H₂₈N₅O₃Cl·(C₄H₈O₂)_{1/4}) C, H, N, Cl.

General Reductive Amination Procedure for 11. Method B: 7-Chloro-4,5-dihydro-5-[(1-(*cis*-3,5,4-trimethyl)piperazino)carbonyl]imidazo[1,5-*a*]quinoxaline-3-carboxylic Acid 1,1-Dimethylethyl Ester (47**).** Sodium cyanoborohydride (351 mg, 5.59 mmol) was added to a mixture of **46** (0.859 g, 1.93 mmol), MeOH (12 mL), and formalin (2.8 mL). The solution was stirred for 16 h at room temperature and was concentrated. Basic workup (CH₂Cl₂, NaHCO₃, MgSO₄) gave a foam which was crystallized from ether/hexane to give 0.813 g (two crops, 92%) of **47** as a tan powder (mp 172–173 °C): IR (mineral oil) 1694, 1688, 1669, 1505, 1274, 1153, 965 cm⁻¹; ¹H NMR (300 MHz, CDCl₃) δ 7.99 (s, ArH), 7.44 (d, *J* = 8.6 Hz, ArH), 7.19 (s, ArH), 7.13 (dd, *J* = 7.7, 1.5

Hz, ArH), 4.94 (s, ArNCH₂), 3.60 (d, $J = 13.0$ Hz, 2 H), 2.73 (apparent t, $J = 12.3$ Hz, 2 H), 2.27 (s, NCH₃), 2.15–2.35 (m, 2 H), 1.63 (s, 'Bu), 1.05 (d, $J = 6.2$ Hz, CHCH₃, 6 H); MS (EI) m/e 459, 403, 248, 230, 155, 141, 127, 113, 98, 86. Anal. (C₂₃H₃₀N₅O₃Cl·(H₂O)_{1/2}) C, H, N, Cl.

7-Chloro-5-(chlorocarbonyl)-4,5-dihydroimidazo[1,5-*a*]quinoxaline-3-carboxylic Acid 1,1-Dimethylethyl Ester (7c). Triphosgene (1.60 g, 5.40 mmol) was added to a solution of **6c** (3.00 g, 9.81 mmol) and diisopropylethylamine (2.1 mL, 12 mmol) in CH₂Cl₂ (81 mL) at 0 °C. The solution was stirred at 0 °C for 1 h and then at room temperature for 1 h. Water (5 mL) was added and the mixture concentrated. Basic workup (EtOAc, dilute NaHCO₃, MgSO₄) gave an oil which was triturated in 10% EtOAc/hexane. The resulting solids were filtered, washed with hexane, and dried to give 3.32 g (92%) of the desired compound as an off-white solid: ¹H NMR (300 MHz, CDCl₃) δ 8.04 (s, ArH), 7.87 (br s, ArH), 7.53 (d, $J = 8.6$ Hz, ArH), 7.35–7.45 (m, ArH), 5.46 (narrow s, ArNCH₂), 1.64 (s, 'Bu).

Example Procedure for the Reaction of Carbamoyl Chloride 7 with an Amine. Method C: (3*R*)-7-Chloro-4,5-dihydro-5-[(1-(3-methyl-4-*tert*-butyloxycarbonyl)piperazino)carbonyl]imidazo[1,5-*a*]quinoxaline-3-carboxylic Acid 1,1-Dimethylethyl Ester (9c; R¹ = 3(*R*)-Me, R² = H). The carbamoyl chloride **7c** (1.03 g, 2.80 mmol) was added to a solution of *tert*-butyl (*R*)-2-methyl-1-piperazinecarboxylate^{25a} (600 mg, 3.00 mmol), diisopropylethylamine (0.70 mL, 4.0 mmol), and CH₂Cl₂ (25 mL) at 0 °C. The solution was stirred at 0 °C for 1 h and at room temperature for 16 h. Basic workup (CH₂Cl₂, NaHCO₃, MgSO₄) and purification by flash chromatography (2:1 EtOAc:hexane) gave 1.32 g (88%) of the desired product as a foam which was carried on crude: IR (mineral oil) 1727, 1695, 1670, 1508, 1409, 1392, 1367, 1167, 1152 cm⁻¹; ¹H NMR (300 MHz, CDCl₃) δ 8.02 (s, ArH), 7.47 (d, $J = 8.6$ Hz, ArH), 7.23 (s, ArH), 7.16 (dd, $J = 8.4, 1.5$ Hz, ArH), 4.97 (AB_q, $J_{AB} = 16.9$ Hz, $\Delta\gamma = 109.9$ Hz, ArNCH₂), 4.20–4.35 (m, 1 H), 3.78 (d, $J = 13.8$ Hz, 1 H), 3.55–3.70 (m, 2 H), 3.00–3.20 (m, 2 H), 2.85–3.00 (m, 1 H), 1.62 (s, ArCO₂'Bu), 1.45 (s, NCO₂'Bu), 1.16 (d, $J = 6.8$ Hz, CHCH₃); MS (EI) m/e 531, 475, 419, 402, 248, 230, 171, 127.

Example Procedure for Deprotection of *tert*-Butyloxycarbonyl 9 to Provide 10. Method D: (3*R*)-7-Chloro-4,5-dihydro-5-[(1-(3-methyl)piperazino)carbonyl]imidazo[1,5-*a*]quinoxaline-3-carboxylic Acid 1,1-Dimethylethyl Ester (90). A solution of 1.29 g (2.42 mmol) of **9c** (R¹ = 3(*R*)-Me, R² = H), CH₂Cl₂ (20 mL), and TFA (12 mL) was stirred at 0 °C for 1 h and concentrated. Basic workup (CH₂Cl₂, NaHCO₃, MgSO₄) gave 902 mg of the product as a foam which was crystallized from EtOAc/ether/hexane to give 793 mg (76%) of **90** as a white powder (mp 157–159 °C), >98% ee by HPLC analysis:²⁷ [α]_D²⁵ +3° ($c = 0.75$, CHCl₃); IR (mineral oil) 1691, 1641, 1512, 1159, 1152 cm⁻¹; ¹H NMR (300 MHz, CDCl₃) δ 8.00 (s, ArH), 7.46 (d, $J = 8.4$ Hz, ArH), 7.10–7.35 (m, ArH), 4.95 (s, ArNCH₂), 3.60–3.80 (m, 2 H), 2.75–3.10 (m, 4 H), 2.62 (t, $J = 10.7$ Hz, 1 H), 1.63 (s, 'BuO), 1.07 (d, $J = 6.1$ Hz, CHCH₃); MS (EI) m/e 431, 375, 318, 248, 230, 203, 179, 127. Anal. (C₂₁H₂₆N₅O₃Cl·(H₂O)_{1/2}) C, H, N, Cl.

7-Chloro-5-[(1-(4-acetyl-*cis*-3,5-dimethyl)piperazino)carbonyl]-4,5-dihydroimidazo[1,5-*a*]quinoxaline-3-carboxylic Acid 1,1-Dimethylethyl Ester (71). Acetyl chloride (0.10 mL, 1.4 mmol) was added to a mixture of **46** (0.600 g, 1.35 mmol), diisopropylethylamine (0.41 mL, 2.4 mmol), and CH₂Cl₂ (15.0 mL). The mixture was allowed to warm to room temperature and stir for 16 h. Basic workup (CH₂Cl₂, 1 N KHCO₃, Na₂SO₄) and purification by crystallization (ether) gave 0.57 g (87%) of **71** as an off-white powder (mp 154–154.5 °C): IR (mineral oil) 1687, 1678, 1668, 1632, 1511, 1420, 1413, 1409, 1391, 1366, 1348, 1335, 1149 cm⁻¹; ¹H NMR (300 MHz, CDCl₃) δ 8.00 (s, ArH), 7.48 (d, $J = 8.5$ Hz, ArH), 7.17 (dd, $J = 10.6, 2.0$ Hz, ArH), 7.11 (narrow m, ArH), 5.00 (s, ArNCH₂), 3.55–3.80 (br s, 2 H), 3.00–3.20 (m, 2 H), 2.11 (s, COCH₃), 1.63 (s, C(CH₃)₃), 1.15–1.40 (m, CHCH₃, 6 H); MS (EI) m/e 487, 431, 248, 231, 230, 141. Anal. (C₂₄H₃₀N₅O₄) C, H, N, Cl.

7-Chloro-4,5-dihydro-5-[(1-(4-methanesulfonyl-*cis*-3,5-dimethyl)piperazino)carbonyl]imidazo[1,5-*a*]quinoxaline-3-carboxylic Acid 1,1-Dimethylethyl Ester (72). Methanesulfonyl chloride (0.15 mL, 1.9 mmol) was added to a mixture of **46** (0.600 g, 1.35 mmol), diisopropylethylamine (0.61 mL, 3.5 mmol), and CH₂Cl₂ (15.0 mL) at 0 °C. The mixture was allowed to warm to room temperature and stir for 80 h. Basic workup (CH₂Cl₂, 1 N KHCO₃, Na₂SO₄) and purification by flash chromatography (1% CH₃OH/CH₂Cl₂) gave 0.439 g (62%) of **72** as a brown foam (mp 156–157 °C): IR (mineral oil) 1724, 1667, 1508, 1423, 1325, 1305, 1281, 1248, 1152, 1126, 964 cm⁻¹; ¹H NMR (300 MHz, CDCl₃) δ 8.00 (s, ArH), 7.48 (d, $J = 8.6$ Hz, ArH), 7.17 (dd, $J = 8.6, 1.5$ Hz, ArH), 7.10 (narrow m, ArH), 4.99 (s, ArNCH₂), 4.00–4.20 (m, 2 H), 3.61 (d, $J = 13.3$ Hz, 2 H), 3.17 (dd, $J = 14.6, 6.1$ Hz, 2 H), 2.88 (s, SO₂CH₃), 1.62 (s, C(CH₃)₃), 1.37 (d, $J = 7.0$ Hz, CHCH₃, 6 H); MS (EI) m/e 523, 467, 450, 248, 232, 231, 230, 219, 136. Anal. (C₂₃H₃₀N₅ClO₅S·(H₂O)_{1/3}) C, H, N, Cl.

6-Chloro-3,3-dimethyl-1,2,3,4-tetrahydro-4-[(1-(*cis*-3,5-dimethyl)piperazino)carbonyl]quinoxalin-2-one (13g; R¹ = R² = *cis*-3,5-dimethyl, R = H). A solution of carbamyl chloride **12g**¹³ (14.2 mmol), CH₂Cl₂ (40 mL), and diisopropylethylamine (2.7 mL, 16 mmol) was cooled to 0 °C. To this was added *cis*-2,6-dimethylpiperazine (2.28 g, 20.0 mmol) as a solid. The solution was stirred at 0 °C for 1 h and for 16 h at room temperature. Basic workup (CH₂Cl₂, NaHCO₃, MgSO₄) and purification by flash chromatography (6:1 ethyl acetate:MeOH) gave 3.86 g of the urea as a foam. Crystallization from ethyl acetate/hexane gave 2.68 g (54%) of the product as a pale yellow powder (mp 151–156 °C): IR (mineral oil) 1697, 1684, 1672, 1648, 1502, 1451, 1235 cm⁻¹; ¹H NMR (300 MHz, CDCl₃) δ 9.27 (s, NH, rotamer), 9.19 (s, NH, rotamer), 6.93 (dd, $J = 8.3, 2.1$ Hz, ArH), 6.75–6.90 (m, ArH), 6.55 (d, $J = 2.0$ Hz, ArH), 4.41 (d, $J = 13.0$ Hz, 1 H), 3.48 (d, $J = 13.0$ Hz, 1 H), 2.60–3.00 (m, 2 H), 2.25–2.55 (m, 2 H), 1.73 (s, CCH₃), 1.30–1.85 (m, NH), 1.44 (s, CCH₃), 1.14 (d, $J = 6.2$ Hz, CHCH₃), 0.95 (d, $J = 6.2$ Hz, CHCH₃); MS (EI) m/e 350, 141, 84, 72.

Example Procedure for Cyclization of 13 with *tert*-Butyl Isocyanacetate to Give 10. Method E: 7-Chloro-4,4-dimethyl-4,5-dihydro-5-[(1-(*cis*-3,5-dimethyl)piperazino)carbonyl]imidazo[1,5-*a*]quinoxaline-3-carboxylic Acid 1,1-Dimethylethyl Ester (57). Potassium *tert*-butoxide (3.00 mL, 3.00 mmol, 1.0 M in THF) was added to a solution of **13g** (R¹ = R² = *cis*-3,5-dimethyl, R = H; 1.00 g, 2.85 mmol) and THF (10 mL) at 0 °C. The solution was stirred at 0 °C for 30 min, and diethyl chlorophosphate (0.44 mL, 3.0 mmol) was added. The solution was allowed to warm to room temperature and stir for 30 min. The solution was cooled to -7 °C, and a solution of the *tert*-butyl isocyanacetate (466 mg, 3.30 mmol) and THF (1.0 mL) was added. Potassium *tert*-butoxide (3.0 mL, 3.0 mmol) was added dropwise over several min. The solution was stirred at 0 °C for 1.5 h and allowed to warm to room temperature and stir for 2 h. Aqueous workup (ethyl acetate, MgSO₄) and purification by flash chromatography (10:1 ethyl acetate:MeOH) gave 1.10 g of an oil which was crystallized from ether/hexane to give 631 mg (47%) of **57** as a white powder (mp 171–175 °C): IR (mineral oil) 1673, 1663, 1510, 1421, 1363, 1254, 1233, 1151, 1142 cm⁻¹; ¹H NMR (300 MHz, CDCl₃) δ 7.96 (s, ArH), 7.39 (dd, $J = 8.4, 1.5$ Hz, ArH), 6.95–7.05 (m, ArH), 6.63 (narrow m, ArH), 4.40–4.55 (m, 1 H), 3.35–3.50 (m, 1 H), 2.60–2.95 (m, 2 H), 2.20–2.55 (m, 2 H), 2.08 (s, CCH₃), 1.90–2.10 (m, 1 H), 1.70 (s, CCH₃), 1.63 (s, 'Bu), 1.14 (d, $J = 6.1$ Hz, CHCH₃), 0.93 (d, $J = 6.9$ Hz, CHCH₃); MS (EI) m/e 474, 473, 458, 402, 345, 244, 141. Anal. (C₂₄H₃₂N₅O₃Cl) C, H, N, Cl.

***N,N*-Dibenzyl-2-nitro-4-trifluoromethylaniline (16).** A solution of 4-chloro-3-nitrobenzotrifluoride (**15**, 10.0 mL, 67.0 mmol), dibenzylamine (25.0 mL, 130 mmol), and diisopropylethylamine (15.0 mL, 86.1 mmol) was heated at 140 °C for 5 h. The solution was allowed to cool and stir overnight at room temperature. The reaction mixture was partitioned between ether (500 mL) and water (250 mL). The organic layer was separated, washed with water (250 mL), and partitioned with water (300 mL). Concentrated HCl was added until the

aqueous layer was pH 1 (pH paper). The dibenzylamine hydrochloride byproduct was removed by filtration, and the two layers were separated. The organic layer was washed with water (200 mL) and brine (2 × 100 mL), dried (MgSO₄), and concentrated to give 25.2 g (97%) of **16** as an orange solid. This material was used in the next step without further purification: IR (mineral oil) 1621, 1532, 1323, 1268, 1164, 1134 cm⁻¹; ¹H NMR (300 MHz, CDCl₃) δ 8.07 (narrow m, ArH), 7.56 (dd, *J* = 8.8, 2.1 Hz, ArH), 7.05–7.40 (m, ArH, 11 H), 4.30 (s, NCH₂, 4 H); MS (EI) *m/e* 386, 369, 295, 263, 248, 91.

2-Dibenzylamino-5-trifluoromethylaniline (17). Hydrazine monohydrate (15.8 mL, 326 mmol) was added dropwise to a stirred mixture of **16** (25.2 g, 65.2 mmol), EtOH (250 mL), and Raney nickel (Aldrich, ca. 6.3 g) at 0 °C. The mixture was stirred at 0 °C for 1 h and then at room temperature overnight. Aqueous workup (ether, brine wash, MgSO₄) gave 23.0 g (99%) of a brown oil which was used without further purification in the next step: ¹H NMR (300 MHz, CDCl₃) δ 7.15–7.40 (m, ArH, 10 H), 6.95 (s, ArH), 6.86 (d, *J* = 1.1 Hz, ArH, 2 H), 4.24 (s, NH₂), 4.08 (s, NCH₂, 4 H).

N-(2-Dibenzylamino-5-trifluoromethylphenyl)glycine Ethyl Ester (18). A solution of **17** (22.3 g, 62.6 mmol), diisopropylethylamine (24.0 mL, 138 mmol), and ethyl bromoacetate (20.9 mL, 188 mmol) was heated at 120 °C for 1 h. The mixture was allowed to cool to room temperature. Aqueous workup (EtOAc, brine wash, MgSO₄) and purification by flash chromatography (1→10% EtOAc/hexane) gave a solid which was triturated in hexane to provide 19.5 g (70%) of **18** as a white solid (mp 85–87 °C): IR (mineral oil) 1740, 1211, 1178, 1170, 1102, 1089 cm⁻¹; ¹H NMR (300 MHz, CDCl₃) δ 7.20–7.35 (m, ArH, 10 H), 6.80–6.95 (m, ArH, 2 H), 6.67 (s, ArH), 5.72 (br s, NH), 4.30 (q, *J* = 7.1 Hz, CH₂CH₃), 4.06 (s, NCH₂-Ar, 4 H), 3.93 (s, CH₂CO₂Et), 1.32 (t, *J* = 7.2 Hz, CH₂CH₃); MS (EI) *m/e* 442, 351, 277, 187, 91.

3,4-Dihydro-2-hydroxy-6-trifluoromethylquinoxaline (19). A mixture of **18** (14.6 g, 33.0 mmol), ethanol (600 mL), and palladium hydroxide on carbon (3.65 g) was hydrogenated at 40 psi for 3 days. The mixture was filtered and concentrated. Basic workup (EtOAc, NaHCO₃, MgSO₄) of the residue gave 6.94 g (97%) of **19** as a white solid (mp 97–98 °C): IR (mineral oil) 1688, 1672, 1424, 1324, 1315, 1252, 1132, 1111 cm⁻¹; ¹H NMR (300 MHz, CDCl₃) δ 9.31 (br s, OH), 7.01 (d, *J* = 7.3 Hz, ArH), 6.89 (s, ArH), 6.83 (d, *J* = 8.1 Hz, ArH), 4.06 (s, NCH₂); MS (EI) *m/e* 216, 187, 167, 140, 91. Anal. (C₉H₇N₂OF₃·(H₂O)_{1/2}) C, H, N.

4,5-Dihydro-7-trifluoromethylimidazo[1,5-*a*]quinoxaline-3-carboxylic Acid 1,1-Dimethylethyl Ester (20). Potassium *tert*-butoxide (35.0 mL, 35.0 mmol, 1.0 M in THF) was added to a mixture of **19** (6.30 g, 29.1 mmol) and THF (100 mL) at -40 °C. The solution was stirred at -40 °C for 10 min and then at room temperature for 30 min. The solution was cooled to -50 °C and diethyl chlorophosphate (5.5 mL, 38 mmol) added. The solution was stirred at -50 °C for 10 min and then at room temperature for 40 min. The solution was cooled to -78 °C, and *tert*-butyl isocynoacetate (5.1 mL, 35 mmol) was added dropwise over several minutes. The solution was allowed to warm slowly and was stirred at room temperature for 4 days. Water (10 mL) was added and the mixture concentrated. Aqueous workup (EtOAc, MgSO₄) and trituration in 20% EtOAc/hexane gave 4.13 g of the desired material as a white solid (mp 242–244 °C). Concentration of the mother liquor and purification by flash chromatography (20% EtOAc/CH₂Cl₂) followed by trituration in 20% EtOAc/hexane gave an additional 619 mg of **20**. The total yield of **20** was 4.75 g (48%): IR (mineral oil) 1704, 1329, 1295, 1247, 1167, 1157, 1115, 1049 cm⁻¹; ¹H NMR (300 MHz, CDCl₃) δ 8.03 (s, ArH), 7.48 (d, *J* = 8.3 Hz, ArH), 7.09 (d, *J* = 8.3 Hz, ArH), 7.03 (narrow m, ArH), 4.86 (s, NCH₂), 1.62 (s, ^tBu); MS (EI) *m/e* 339, 283, 266, 237, 186. Anal. (C₁₆H₁₆N₃O₂F₃) C, H, N.

***tert*-Butyl *cis*-3,5-Dimethyl-1-piperazinecarboxylate (30)**. A solution of di-*tert*-butyl dicarbonate (11.8 g, 54.1 mmol) and CH₂Cl₂ (30 mL) was added dropwise over 15 min to a solution of *cis*-2,6-dimethylpiperazine **29** (6.25 g, 54.7 mmol)

and CH₂Cl₂ (120 mL) at 0 °C. The solution was stirred for 1 h at 0 °C and 16 h at room temperature. Aqueous workup (CH₂-Cl₂, K₂CO₃) gave 10.9 g (93%) of **30** as a viscous oil, homogeneous by TLC analysis: ¹H NMR (300 MHz, CDCl₃) δ 3.7–4.2 (m, 2 H), 2.7–2.85 (m, 2 H), 2.2–2.45 (m, 2 H), 1.46 (s, ^tBuO), 1.06 (d, *J* = 6.3 Hz, CHCH₃, 6 H).

***tert*-Butyl 4-Isopropyl-*cis*-3,5-dimethyl-1-piperazine-carboxylate (31)**. A mixture of **30** (10.9 g, 50.9 mmol), 2-iodopropane (50 mL), acetonitrile (100 mL), and K₂CO₃ (15.0 g, 109 mmol) was heated at reflux for 5 days. Additional 2-iodopropane (25 mL), K₂CO₃ (15 g, 109 mmol), and acetonitrile (25 mL) were added after 2 days. After cooling to room temperature, aqueous workup (CH₂Cl₂, MgSO₄) and purification by flash chromatography (10:1 ethyl acetate:MeOH) gave 5.39 g (41%) of **31** as an oil: ¹H NMR (300 MHz, CDCl₃) δ 3.35–3.50 (m, 2 H), 3.10–3.30 (m, 3 H), 2.85–3.05 (m, 2 H), 1.46 (s, ^tBuO), 1.05 (d, *J* = 6.4 Hz, CHCH₃, 6 H), 1.04 (d, *J* = 6.7 Hz, CHCH₃, 6 H).

1-Isopropyl-*cis*-2,6-dimethylpiperazine (32). A solution of **31** (780 mg, 3.04 mmol), CH₂Cl₂ (10.0 mL), and trifluoroacetic acid (10.0 mL) was stirred for 1 h at 0 °C and concentrated. Basic workup (CH₂Cl₂, 20% NaOH, K₂CO₃) gave 427 mg (90%) of **32** as an oil: ¹H NMR (300 MHz, CDCl₃) δ 3.15–3.30 (m, CH(CH₃)₂), 2.80–2.90 (m, 2 H), 2.50–2.70 (m, 4 H), 1.30–1.70 (m, NH), 1.12 (d, *J* = 7.0 Hz, 6 H), 1.06 (d, *J* = 5.9 Hz, 6 H).

(S)-[2-[(2-Hydroxyethyl)amino]-1-methyl-2-oxoethyl]-carbamic Acid 1,1-Dimethylethyl Ester (34A). CDI (3.44 g, 21.2 mmol) was added to a solution of Boc-L-alanine **33** (4.00 g, 21.1 mmol) and CH₂Cl₂ (64 mL). The solution was stirred for 1 h at room temperature. Ethanolamine (1.30 mL, 21.5 mmol) was then added. The solution was stirred for 70 h at room temperature and then concentrated. Purification by flash chromatography (9:1 EtOAc:MeOH) gave 4.13 g (84%) of **34A** as an oil: IR (neat) 3308, 1694, 1659, 1531, 1368, 1169 cm⁻¹; ¹H NMR (300 MHz, CDCl₃) δ 6.55–6.70 (m, 1 H), 4.90–5.10 (m, 1 H), 4.12 (q, *J* = 6.9 Hz, NCHCH₃), 3.72 (t, *J* = 5.0 Hz, NCH₂CH₂OH), 3.35–3.55 (m, NCH₂CH₂), 1.45 (s, ^tBuO), 1.38 (d, *J* = 7.1 Hz, CHCH₃); MS (EI) *m/e* 232, 202, 176, 159, 144, 113, 102, 88.

(S)-[2-[(2-Hydroxyethyl)amino]-1-methylethyl]carbamic Acid 1,1-Dimethylethyl Ester (35A). Borane–methyl sulfide complex (3.00 mL, 30.0 mmol, 10.0 M) was added to a solution of **34A** (2.77 g, 11.9 mmol) and THF (70 mL). The solution was stirred for 16 h at room temperature, and the reaction was quenched slowly with 10% HCl. THF (100 mL), water (25 mL), and KOH (4.00 g) were added, and the mixture was heated at reflux for 24 h. After the mixture cooled to room temperature, the organic layer was removed under reduced pressure. The aqueous layer was saturated with sodium chloride and extracted several times with CH₂Cl₂. The organic layers were dried (K₂CO₃), filtered, and concentrated to give 1.72 g (66%) of **35A** as a white solid (mp 54–58 °C) sufficiently pure to be carried on crude: [α]_D²⁵ -3° (*c* = 1.0, CHCl₃); IR (mineral oil) 3355, 1681, 1519, 1366, 1165, 1073 cm⁻¹; ¹H NMR (300 MHz, CDCl₃) δ 4.50–4.65 (m, 1 H), 3.60–3.90 (m, 1 H), 3.63 (t, *J* = 5.4 Hz, CH₂O), 2.75–2.90 (m, 2 H), 2.55–2.70 (m, 2 H), 1.50–2.10 (m, OH, NH), 1.45 (s, ^tBu), 1.14 (d, *J* = 6.7 Hz, CHCH₃); MS (EI) *m/e* 200, 187, 145, 131, 101, 74.

(S)-7-Chloro-5-[[[2-[[[(1,1-dimethylethoxy)carbonyl]amino]propyl](2-hydroxyethyl)amino]carbonyl]-4,5-dihydroimidazo[1,5-*a*]quinoxaline-3-carboxylic Acid 1,1-Dimethylethyl Ester (36A; R⁷ = Cl). The carbamoyl chloride **7c** (1.32 g, 3.58 mmol) was added to a solution of **35A** (858 mg, 3.93 mmol), diisopropylethylamine (0.90 mL, 5.2 mmol), and CH₂Cl₂ (25 mL) at 0 °C. The solution was stirred at 0 °C for 1 h and at room temperature for 16 h. Basic workup (CH₂-Cl₂, NaHCO₃, MgSO₄) and purification by flash chromatography (EtOAc) gave 1.58 g (80%) of **36A** as a tan foam which was carried on crude (mp 118–122 °C): IR (mineral oil) 1723, 1710, 1510, 1250, 1157 cm⁻¹; ¹H NMR (300 MHz, CDCl₃) δ 7.97 (s, ArH), 7.43 (d, *J* = 8.6 Hz, ArH), 7.39 (s, ArH), 7.12 (dd, *J* = 6.9, 1.5 Hz, ArH), 4.92 (AB_q, *J*_{AB} = 15.3 Hz, Δγ = 28.0 Hz, ArNCH₂), 4.55–4.70 (m, 1 H), 3.70–4.00 (m, 3 H),

3.30–3.60 (m, 3 H), 3.11 (dd, $J = 14.6, 6.1$ Hz, 1 H), 2.65–2.85 (m, 1 H), 1.61 (s, ArCO₂tBu), 1.43 (s, NCO₂tBu), 1.05 (d, $J = 6.6$ Hz, CHCH₃); MS (EI) m/e 549, 493, 437, 350, 248, 230, 203, 189, 145.

(S)-5-[(2-aminopropyl)(2-hydroxyethyl)amino]carbonyl]-7-chloro-4,5-dihydroimidazo[1,5-a]quinoxaline-3-carboxylic Acid 1,1-Dimethylethyl Ester (37A; R⁷ = Cl). A solution of **36A** (R⁷ = Cl; 1.54 g, 2.80 mmol), CH₂Cl₂ (22 mL), and TFA (14 mL) was stirred at 0 °C for 1 h and then concentrated. Basic workup (CH₂Cl₂, NaHCO₃, MgSO₄) gave 956 mg (76%) of **37A** (R⁷ = Cl) as a foam which was carried on crude: ¹H NMR (300 MHz, CDCl₃) δ 7.99 (s, ArH), 7.44 (d, $J = 8.6$ Hz, ArH), 7.21 (d, $J = 2.3$ Hz, ArH), 7.10–7.20 (m, ArH), 4.93 (AB_q, $J_{AB} = 15.3$ Hz, $\Delta\gamma = 83.6$ Hz, ArNCH₂), 3.65–3.75 (m, 2 H), 3.25–3.55 (m, 5 H), 1.60 (s, tBuO), 1.17 (d, $J = 6.4$ Hz, CHCH₃).

Example Procedure for Intramolecular Mitsunobu Cyclization of an Amino Alcohol to Piperazine 10. **Method F: (3S)-7-Chloro-4,5-dihydro-5-[(1-(3-methylpiperazino)carbonyl)imidazo[1,5-a]quinoxaline-3-carboxylic Acid 1,1-Dimethylethyl Ester (89).** Diethyl azodicarboxylate (DEAD, 0.43 mL, 2.7 mmol) was added to a solution of **37A** (R⁷ = Cl; 951 mg, 2.11 mmol), triphenylphosphine (745 mg, 2.84 mmol), and THF (18.6 mL). The solution was stirred at room temperature for 16 h and then concentrated. Purification by flash chromatography (4:1 EtOAc:MeOH) gave the product as a foam which was crystallized from EtOAc/ether/hexane to give 542 mg (59%, two crops) of **89** as a white powder (mp 158–160 °C), >98% ee by HPLC analysis:²⁷ [α]_D²⁵ –1° ($c = 0.92$, EtOH); IR (mineral oil) 1687, 1646, 1611, 1511, 1435, 1423, 1390, 1359, 1311, 1295, 1282, 1154, 1133, 968 cm⁻¹; ¹H NMR (300 MHz, CDCl₃) δ 7.99 (s, ArH), 7.45 (d, $J = 8.6$ Hz, ArH), 7.21 (s, ArH), 7.13 (dd, $J = 8.5, 2.1$ Hz, ArH), 4.95 (s, ArNCH₂), 3.60–3.80 (m, 2 H), 2.75–3.00 (m, 4 H), 2.55 (dd, $J = 12.6, 10.6$ Hz, 1 H), 1.63 (s, tBu), 1.04 (d, $J = 6.3$ Hz, CHCH₃); MS (EI) m/e 431, 375, 358, 317, 248, 230, 203, 179, 127. Anal. (C₂₁H₂₆N₅O₃Cl·(H₂O)_{4/5}) C, H, N, Cl.

(S)-[2-[(2(R)-Hydroxypropyl)amino]-1-methyl-2-oxoethyl]carbamic Acid 1,1-Dimethylethyl Ester (34B). CDI (3.44 g, 21.2 mmol) was added to a solution of Boc-L-alanine (4.00 g, 21.1 mmol) and CH₂Cl₂ (64 mL). The solution was stirred for 1 h at room temperature and then (R)-1-amino-2-propanol (2.50 mL, 31.8 mmol) was added. The solution was stirred for 16 h at room temperature and then concentrated. Purification by flash chromatography (EtOAc) gave 4.60 g (89%) of **34B** as a clear oil: IR (neat) 3308, 2978, 1694, 1659, 1530, 1368, 1250, 1170 cm⁻¹; ¹H NMR (300 MHz, CDCl₃) δ 6.45–6.60 (m, 1 H), 4.85–5.00 (m, 1 H), 4.13 (q, $J = 6.9$ Hz, NCHCH₃), 3.90–4.00 (m, 1 H), 3.35–3.50 (m, 1 H), 3.05–3.20 (m, 1 H), 1.45 (s, tBuO), 1.38 (d, $J = 7.1$ Hz, CHCH₃), 1.19 (d, $J = 6.3$ Hz, CHCH₃); MS (EI) m/e 202, 173, 144, 102, 88.

(S)-[2-[(2(R)-Hydroxypropyl)amino]-1-methylethyl]carbamic Acid 1,1-Dimethylethyl Ester (35B). Borane–methyl sulfide complex (4.70 mL, 47.0 mmol, 10.0 M) was added to a solution of **34B** (4.54 g, 18.4 mmol) and THF (110 mL). The solution was stirred for 16 h at room temperature and then quenched slowly with 10% HCl. Water (40 mL) and KOH (10.0 g) were added, and the mixture heated at reflux for 26 h. After cooling to room temperature, the organics were removed under reduced pressure. The aqueous layer was saturated with sodium chloride which was extracted several times with CH₂Cl₂. The organic layers were dried (MgSO₄), filtered, and concentrated to give 3.22 g (75%) of **35B** as a white solid, sufficiently pure to be carried on crude. A small portion was recrystallized from hot ether/hexane to give a white crystalline material (mp 77–78 °C): [α]_D²⁵ –28° ($c = 0.98$, CHCl₃); IR (mineral oil) 3374, 1683, 1525, 1177, 1160, 1093 cm⁻¹; ¹H NMR (300 MHz, CDCl₃) δ 4.45–4.65 (m, 1 H), 3.65–3.90 (m, 2 H), 2.50–2.85 (m, 3 H), 2.40 (dd, $J = 12.0, 9.4$ Hz, 1 H), 2.05–2.50 (m, NH, OH), 1.45 (s, tBuO), 1.15 (d, $J = 6.2$ Hz, CHCH₃), 1.14 (d, $J = 6.7$ Hz, CHCH₃); MS (EI) m/e 214, 187, 159, 141, 131, 115, 88.

[R-(R*,S*)]-7-Chloro-5-[[[2-[(1,1-dimethylethoxy)carbonyl]amino]propyl](2-hydroxypropyl)amino]carbonyl]-

4,5-dihydroimidazo[1,5-a]quinoxaline-3-carboxylic Acid 1,1-Dimethylethyl Ester (36B, R⁷ = Cl). The carbamoyl chloride **7c** (1.51 g, 4.10 mmol) was added to a solution of **35B** (1.05 g, 4.52 mmol), diisopropylethylamine (1.03 mL, 5.91 mmol), and CH₂Cl₂ (33 mL) at 0 °C. The solution was stirred at 0 °C for 1 h and at room temperature for 5 h. Basic workup (CH₂Cl₂, NaHCO₃, MgSO₄) and purification by flash chromatography (EtOAc) gave 1.79 g (77%) of **36B** (R⁷ = Cl) as a pale yellow powder which was carried on crude: IR (mineral oil) 1724, 1710, 1657, 1510, 1416, 1251, 1159, 1151, 1127 cm⁻¹; ¹H NMR (300 MHz, CDCl₃) δ 7.99 (s, ArH), 7.52 (narrow m, ArH), 7.43 (d, $J = 8.6$ Hz, ArH), 7.11 (dd, $J = 9.2, 1.5$ Hz, ArH), 4.92 (s, ArNCH₂), 4.45–4.60 (m, 1 H), 4.05–4.25 (m, 1 H), 3.80–4.00 (m, 1 H), 3.05–3.50 (m, 4 H), 1.61 (s, ArCO₂tBu), 1.43 (s, NCO₂tBu), 1.18 (d, $J = 6.2$ Hz, CHCH₃), 1.02 (d, $J = 6.7$ Hz, CHCH₃); MS (EI) m/e 563, 451, 434, 364, 276, 248, 230, 203, 159, 141.

[R-(R*,S*)]-5-[[[2-Aminopropyl](2-hydroxypropyl)amino]carbonyl]-7-chloro-4,5-dihydroimidazo[1,5-a]quinoxaline-3-carboxylic Acid 1,1-Dimethylethyl Ester (37B, R⁷ = Cl). A solution of **36B** (R⁷ = Cl; 1.77 g, 3.14 mmol), CH₂Cl₂ (25 mL), and TFA (16 mL) was stirred at 0 °C for 1 h and then concentrated. Basic workup (CH₂Cl₂, NaHCO₃, MgSO₄) gave 1.07 g (73%) of **37B** (R⁷ = Cl) as a pale yellow foam which was carried on crude: IR (mineral oil) 1722, 1695, 1661, 1510, 1417, 1294, 1282, 1216, 1152, 1129 cm⁻¹; ¹H NMR (300 MHz, CDCl₃) δ 7.99 (s, ArH), 7.44 (d, $J = 8.6$ Hz, ArH), 7.23 (narrow m, ArH), 7.13 (dd, $J = 8.4, 2.3$ Hz, ArH), 4.92 (AB_q, $J_{AB} = 15.3$ Hz, $\Delta\gamma = 66.7$ Hz, ArNCH₂), 4.00–4.15 (m, 1 H), 3.30–3.50 (m, 3 H), 3.10–3.30 (m, 1 H), 3.07 (dd, $J = 14.6, 10.0$ Hz, 1 H), 1.62 (s, tBuO), 1.09 (d, $J = 6.1$ Hz, CHCH₃), 1.05 (d, $J = 6.2$ Hz, CHCH₃); MS (EI) m/e 463, 407, 364, 248, 230, 203, 179, 159, 141.

Method F. (3S,5S)-7-Chloro-5-[(1-(3,5-trans-dimethylpiperazino)carbonyl)-4,5-dihydroimidazo[1,5-a]quinoxaline-3-carboxylic Acid 1,1-Dimethylethyl Ester (91). DEAD (0.46 mL, 2.9 mmol) was added to a solution of **37B** (R⁷ = Cl; 1.05 g, 2.26 mmol), triphenylphosphine (800 mg, 3.05 mmol), and THF (20 mL). The solution was stirred at room temperature for 16 h and then concentrated. Purification by flash chromatography (4:1 EtOAc:MeOH) gave 835 mg of **91** as an oil which was crystallized from ether/hexane to give 711 mg (71%, two crops) of the amine as a white powder (mp 121–125 °C), >98% ee by ¹H NMR analysis²⁷ of the Mosher amide:⁵² [α]_D²⁵ +47° ($c = 0.92$, CHCl₃); IR (mineral oil) 1724, 1695, 1662, 1508, 1419, 1295, 1279, 1266, 1243, 1150, 1127 cm⁻¹; ¹H NMR (300 MHz, CDCl₃) δ 7.99 (s, ArH), 7.45 (d, $J = 8.5$ Hz, ArH), 7.10–7.20 (m, ArH, 2 H), 4.95 (AB_q, $J_{AB} = 16.0$ Hz, $\Delta\gamma = 77.9$ Hz, ArNCH₂), 3.30–3.45 (m, 2 H), 3.15–3.30 (m, 2 H), 3.02 (dd, $J = 13.0, 6.1$ Hz, 2 H), 1.62 (s, tBuO), 1.09 (d, $J = 6.5$ Hz, CHCH₃, 6 H); MS (EI) m/e 445, 389, 318, 306, 248, 230, 141. Anal. (C₂₂H₂₈N₅O₃Cl·(H₂O)_{1/3}) C, H, N, Cl.

GABA_A Receptor Expression and Membrane Preparation. DNA manipulations and general baculovirus methods (Sf-9 cell cultivation, infection, and isolation; purification of recombinant viruses) were performed as described elsewhere.²⁹ The Sf-9 cells were infected at a multiplicity of infection of 3 PFU of the following viruses: AcNPV- α_1 , - α_3 , or - α_6 , AcNPV- β_2 , and AcNPV- γ_2 . Infected cells were used for electrophysiological measurements at 48 h postinfection or for membrane preparations at 60 h postinfection. The stable cell lines expressing α_1 , α_3 , or α_6 , β_2 , and γ_2 subunits of GABA_A were derived by transfection of plasmids containing cDNA and a plasmid encoding G418 resistance into human kidney cells (A293 cells) as described elsewhere.³⁰ After 2 weeks of selection in 1 mg/mL G418, cells positive for all three GABA_A receptor mRNAs by Northern blotting were used for electrophysiology to measure GABA-induced Cl⁻ currents.

For equilibrium binding measurements, Sf-9 cells infected with baculovirus-carrying cDNAs for α_1 , α_3 , or α_6 , β_2 , and γ_2 subunits were harvested in 2 L batches at 60 h postinfection. The membranes were prepared following the procedure described previously.²⁹ Briefly, the membranes were prepared in normal saline after homogenization with a Polytron PT 3000

homogenizer (Brinkman) for 4 min. Unbroken cells and large nuclei aggregates were removed by centrifugation at 1000g for 10 min. Then the membranes were recovered with the second centrifugation of the supernatant at 40000g for 50 min. The membranes were resuspended to a final concentration of 5 mg/mL in a solution containing 300 mM sucrose, 5 mM Tris/HCl, pH 7.5, and glycerol to a final concentration of 20% and stored at -80°C . Equilibrium binding of [^3H]flunitrazepam or [^3H]Ro-4513 to the cloned GABA_A receptors was measured in a 500 μL volume of normal saline containing 6 nM [^3H]flunitrazepam or [^3H]Ro-4513, varying concentrations of test ligands, and 50 μg of membrane protein. The mixture was incubated for 60 min at 4°C , filtered over a Whatman glass fiber filter, and washed four times with cold normal saline. The filter was then counted for radioactivity in the presence of a scintillation cocktail (Insta Gel).

GABA_A Receptor Binding. The in vitro binding affinity of the imidazo[1,5-a]quinoxalines for GABA_A was determined as previously described with minor modification.²⁸ Freshly prepared rat cerebellar membranes were suspended in 300 mM sucrose and 10 mM Hepes/Tris, pH 7.4. Typically, the reaction medium contained 6 mM [^3H]flunitrazepam, 50 μg of membrane protein, test drugs at various concentrations or vehicle in 200 μL , 118 mM NaCl, 10 mM Hepes/Tris, pH 7.4, and 1 mM MgCl₂. The mixtures were incubated for 60 min at 4°C . The amount of binding was determined with rapid filtration techniques using Whatman GF/B filters.

[^{35}S]-tert-Butyl Bicyclophosphorothionate ([^{35}S]TBPS) Binding. Binding of [^{35}S]TBPS in the rat brain membranes was measured in the medium containing 2 nM [^{35}S]TBPS, unless specified otherwise, 50 μg of membrane proteins, 1 M NaCl, and 10 mM Tris/HCl, pH 7.4, in a total volume of 500 μL . Drugs were added in concentrated methanolic solutions, and the level of methanol did not exceed 0.2% and was maintained constant in all tubes. The mixtures were incubated for 120 min at 24°C . The reaction mixtures were filtered over a Whatman GF/B filter under vacuum. The filters were washed three times with 4 mL of the reaction buffer without radioisotope and counted for radioactivity. Nonspecific binding was estimated in the presence of 2 μM diazepam or unlabeled TBPS and subtracted to compute specific binding.³³

Electrophysiology. The whole cell configuration of the patch clamp technique was used to record the GABA-mediated Cl⁻ currents in the A293 cells expressing the $\alpha_1\beta_2\gamma_2$ subtype, as described earlier.³⁵ Briefly, patch pipets made of borosilicate glass tubes were fire-polished and showed a tip resistance of 0.5–2 M Ω when filled with a solution containing 140 mM CsCl, 11 mM EGTA, 4 mM MgCl₂, 2 mM ATP, and 10 mM Hepes, pH 7.3. The cell-bathing external solution contained 135 mM NaCl, 5 mM KCl, 1 mM MgCl₂, 1.8 mM CaCl₂, and 5 mM Hepes, pH 7.2 (normal saline). GABA at the concentration of 5 μM in the external solution with or without indicated drugs was applied through a U-tube placed within 100 μM of the cells for 10 s, unless indicated otherwise. The current was recorded with an Axopatch 1D amplifier and a CV-4 headstage (Axon Instrument Co.). A Bh-1 bath headstage was used to compensate for changes in bath potentials. The currents were recorded with a Gould recorder 220. GABA currents were measured at the holding potential of -60 mV at room temperature (21 – 24°C).

Metrazole Antagonism. Compounds were tested for their ability to antagonize metrazole-induced convulsions in rats after ip injection as described elsewhere.³⁷ Briefly, male CF-1 mice were injected with metrazole (85 mg/kg, sc) and convulsive seizure was elicited 15 min later with an auditory stimulation (5 dB for 10 s). Drugs tested for metrazole antagonism were injected ip 30 min before the metrazole challenge, 4 mice/dose at a 0.3 log dose interval. ED₅₀'s for protection against tonic seizure were calculated by the method of Spearman–Karber (Finney, D. J. *Statistical Methods in Biological Assay*).

Ex Vivo Binding Assay. This assay was carried out as previously described with minor modification.^{40a} Briefly, the test drug in vehicle 122 was administered orally to CF-1 mice.

Control mice received an equal volume of the vehicle (1 mL/100 g). Animals were sacrificed at 30, 60, 120, and 240 min after administration of drug. Whole brain minus cerebellum was quickly removed and stored at -78°C until used for the binding assay. Brains were thawed and then homogenized in 50 volumes of cold (4°C) 50 mM Tris-HCl buffer. [^3H]Flunitrazepam binding was determined by incubating 1.0 mL aliquots of the homogenate with 0.1 mL of [^3H]flunitrazepam to give a final concentration of 0.68 nM, 0.1 mL of distilled water or flurazepam (10 μM), and 0.8 mL of 50 mM Tris-HCl buffer, pH 7.4, to give a final volume of 2.0 mL. The mixture was incubated for 30 min at 25°C and then filtered under vacuum through Whatman GF/B filters. The filter and incubation tube were rinsed four times 5 mL aliquots of buffer. The filter paper was placed in a scintillation vial to which 15 mL of ACS (Amersham) cocktail was added. Radioactivity was counted by a liquid scintillation spectrometer. Specific binding was defined as total binding minus binding in the presence of 10 μM flurazepam. Specific binding represented over 95% of total binding. The results are expressed as percent inhibition of (^3H)-FNZ binding, with the ratio calculated as previously described.^{40a}

Cerebellar cGMP Assay. This assay was performed as described previously.⁴² Thus in brief, the test compounds were dissolved in vehicle 122 and administered orally to male CF-1 mice. Control mice received an equal volume of vehicle (1 mL/100 g). Thirty minutes after drug or vehicle treatment, animals were sacrificed and the levels of the cerebellar cGMP determined by the procedure described by Burkard.⁵³ The cerebellum was quickly removed and homogenized in 10 volumes of 1% perchloric acid. The samples were kept on ice for 30 min, boiled for 5 min, and then centrifuged at 17000g for 20 min. The content of cGMP in the supernatant was measured by a radioimmunoassay. Animals in the stressed group were subjected to electric footshock (1.0 mA for 10 s) stress 30 min after drug or vehicle administration. Mice were immediately sacrificed with the levels of cGMP estimated as described above. The results are expressed as percent of control for animals treated with (drug + stress)/stress with statistical analysis done using one-way analysis of variance and subsequently by Student's *t*-test.

Acute Physical Dependence.⁴³ Male CF-1 mice (10/group) were dosed sc twice daily with the test compound, once at 0800 and again at 1600 (with 2 times the 0800 dose) for 3 days. Twenty-four h after the last dose, they received an intravenous injection of the benzodiazepine antagonist flumazenil (2.5 mg/kg in 5% aqueous *N,N*-dimethylacetamide). Five minutes later, the electroshock seizure threshold was estimated by the up-down method in which the stimulus current was lowered or elevated by a 0.05 log interval if the preceding animal did or did not convulse, respectively. From the data thus generated, a threshold (effective current of 50) was calculated. The other parameters of the transpinnal (e.g., delivered across the ears via saline-soaked ear clip electrodes) square wave stimulation were held constant (0.6 ms pulses at 100 Hz for 0.2 s). Test compounds, the precipitated withdrawal from which significantly lowered (below 95% confidence interval of parallel control group treated for 3 days with saline and injected intravenously with flumazenil) the seizure threshold, were considered to have caused physical dependence.

Benzodiazepine Antagonism. Male CF-1 Charles River mice were injected ip simultaneously with 1 mg/kg triazolam and test compound starting at 100 mg/kg. A dose-response was run on a 0.5 log scale. All drugs were made up in No. 122 sterile vehicle (0.25% aqueous methyl cellulose). Fifteen minutes later, they were tested for loss of traction response (muscle relaxation) as indicated above. If the expected loss of traction in response to triazolam was not observed, the test compound was assumed to be an antagonist. Lower doses (at 0.5 log intervals) of the test compound were then evaluated to establish the antagonist dose₅₀ (ED₅₀).

Vogel's Punished Licking Assay. Following a previously reported procedure,^{9a} naive male Fischer 344 rats (except for the 42 experiment which used less responsive Sprague-

Dawley rats) were deprived of water for 48 h prior to lick training in the morning of the test day. Those drinking appreciably in the morning were tested in the afternoon 30 min after ip injection of the test compound, with at least 8 animals/dose group. Drugs were dissolved or suspended in a 0.25% methyl cellulose and saline solution (Upjohn vehicle 122). Training consisted of placement in the chamber for up to 5 min or until rats licked the drinking spout for 1 min. Testing consisted of a 3 min session in which each twentieth lick produced a 0.5 s duration application of distributed electric shock to the grid floor and drinking spout. Data presented are the means and standard errors of the mean of the number of shocks produced in each group by licking. Statistical significance was determined by using a one-way analysis of variance followed by the nonparametric Wilcoxon rank sum test comparing the test dose to that of the contemporaneous vehicle group.

Geller–Cook Conflict Assay. Following a previously reported procedure,^{9a} Sprague–Dawley rats (male) were trained for many weeks to press a lever for food on a MULT VI60/FR10 reinforcement schedule in which a 0.5 s duration footshock was administered with each food pellet during the FR10 components of the schedule. Sessions consisted of four 5-min VI60 components alternating with four 2-min FR10 components. Shock intensity was adjusted to depress responding under the FR10 components to approximately the rate on VI60 components. This generally constituted a halving of FR10 response rate. After performance stabilized, the test drug or vehicle was injected ip 30 min before the session, with at least 6 animals/dose group. A drug effect for each rat was measured by an increase in responding compared to the immediately preceding vehicle session. Statistical significance for each dose was estimated by the Wilcoxon signed-rank test.

Pharmacokinetic Evaluation. Animal Studies. Male Sprague–Dawley rats, surgically prepared with indwelling superior vena cava (SVC) cannulas⁵⁴ were dosed the drug of choice at a nominal dose of 5 mg/kg as an intravenous (iv) bolus via the SVC or as an oral gavage (po). The following week, the rats were administered the same drug at a nominal dose of 5 mg/kg by the opposite route in a crossover fashion. The volume of the dose was based on the weight of the rat on the day of dosing and the measured concentration of the solution formulation. The actual dose for each rat was calculated by weighing the dosing syringe prior to and after the dosing. The rats were fasted overnight prior to and 4 h post to drug administration. Water was available ad libitum. Blood samples (300 μ L) were collected via the SVC before dosing (0 h) and at 2, 5, 10, and 30 min and at 1, 2, 4, 8, and 24 h after iv dosing, and before dosing (0 h) and at 15 and 30 min and 1, 2, 4, 8, and 24 h after po dosing. The blood was allowed to clot at room temperature before centrifugation. The serum was transferred to a clean labeled vial and stored at -15 to -25 °C until assay.

Analytical Methods. Unknown serum samples (100 μ L) were extracted using phenyl solid-phase extraction (SPE) columns (100 mg/0.1 mL Varian Sample Preparation Products, Harbor City, CA) with 1 mL of acetone, followed by 1 mL of acetonitrile as elution solvents. The elution solvents were taken to dryness in a TurboVap LV Evaporator (Zymark Corporation, Hopkinton, MA) set at 40 °C. The drug and IS were redissolved in 300 μ L of acetonitrile/water (30/70, v/v). The redissolved eluates were analyzed by reversed phase high-performance liquid chromatography using a Zorbax SB-CN column (250 mm \times 4.6 mm o.d., 5 μ M particle size, Dupont, Wilmington, DE). The mobile phase was acetonitrile/water (28/72, v/v, for **46**, **47**, and **91**; 25/75, v/v, for **63**; and 35/15, v/v, for **55**) containing 0.1% trifluoroacetic acid by volume. The column effluent was monitored by a Spectra Physics Spectra FOCUS UV detector at 230 nm. Quantitation was accomplished by peak height ratio of the drug to the internal standard using a Harris NightHawk Computer System. The calibration curve, along with a statistical evaluation of standards linear fit, were computed by a linear regression program. The equation $Y \cdot IS = aX$ (forced through the origin) with no

weighting was used to calculate the unknown sample concentrations by inverse prediction against the calibration curve.

Pharmacokinetic Analysis. Selected pharmacokinetic parameters were calculated using model-independent methods.⁵⁵ The maximum serum concentration (C_{max}) and the time at which C_{max} was reached (t_{max}) were obtained from the observed concentration–time data. The area under the serum concentration time curve (AUC) extrapolated to infinity was calculated using the equation $AUC = AUC(0, t_{last}) + C_{t_{last}}/k$, where $AUC(0, t_{last})$ is the area under the curve from time zero to the last time point with a measurable serum concentration ($C_{t_{last}}$), and k , the terminal disposition rate constant, is determined from the linear regression slope of the terminal portion of the log serum concentration–time curve. The terminal disposition half-life ($t_{1/2}$) was obtained from $0.693/k$. Total plasma clearance, Cl_p , was calculated from $Dose_{iv}/AUC_{iv}$ following iv administration. The percent absolute bioavailability (F) was determined by $F = (AUC_{po} \cdot Dose_{iv} \cdot 100\%)/(AUC_{iv} \cdot Dose_{po})$.

References

- (1) (a) Squires, R., Ed. *GABA and Benzodiazepine Receptors*; CRC Press: Boca Raton, FL, 1988; Vol. I, II. (b) Haefely, W. In *Benzodiazepines*; Beaumont, G., Brandon, S., Leonard, B. E., Eds.; John Wiley and Sons: New York, 1990; pp 1–18. (c) Haefely, W. Partial Agonists of the Benzodiazepine Receptor: From Animal Data to Results in Patients. In *Chloride Channels and Their Modulation by Neurotransmitters and Drugs*; Biggio, G., Costa, E., Eds.; Raven Press: New York, 1988; pp 275–292.
- (2) (a) Gardner, C. R. Functional In Vivo Correlates of the Benzodiazepine Agonist-Inverse Agonist Continuum. *Prog. Neurobiol.* **1988**, *31*, 425–476. (b) Braestrup, C.; Nielsen, M. In *Receptor Biochemistry and Methodology*; Olsen, R. W., Venter, J. C., Eds.; A. R. Liss, Inc.: New York, 1986; Vol. 5, p 167. (c) Bare, T. M.; Resch, J. F.; Patel, J. B. Anxiolytics and Sedative-Hypnotics. In *Annual Reports in Medicinal Chemistry*; Bailey, D. M., Ed.; Academic Press: New York, 1987; Vol. 22, pp 11–20. (d) Haefely, W.; Kyburz, E.; Gerecke, M.; Mohler, H. Recent Advances in the Molecular Pharmacology of Benzodiazepine Receptors and in the Structure–Activity Relationships of Their Agonists and Antagonists. In *Advances in Drug Research*; Testa, B., Ed.; Academic Press: New York, 1985; Vol. 14, pp 165–322. (e) Braestrup, C.; Honore, T.; Nielsen, M.; Petersen, E. N.; Jensen, L. H. Ligands for Benzodiazepine Receptors With Positive and Negative Efficacy. *Biochem. Pharmacol.* **1984**, *33*, 859–862.
- (3) (a) Petersen, E. N.; Jensen, L. H.; Diejer, J.; Honore, T. New Perspectives in Benzodiazepine Receptor Pharmacology. *Pharmacopsychiatry* **1986**, *19*, 4–6. (b) Haefely, W. Psychopharmacology of Anxiety. *Eur. Neuropharmacol.* **1991**, *1*, 89–95.
- (4) For recent reviews, see: (a) Gardner, C. R. A Review of Recently-Developed Ligands for Neuronal Benzodiazepine Receptors and Their Pharmacological Activities. *Prog. Neuro-Psychopharmacol. Biol. Psychiatry* **1992**, *16*, 755–781. (b) Gammill, R. B.; Carter, D. B. Neuronal BZD Receptors: New Ligands, Clones and Pharmacology. In *Annual Reports Medicinal Chemistry*; Bristol, J. A., McCall, J. M., Eds.; Academic Press: New York, 1993; Vol. 28, pp 19–27.
- (5) (a) Stephens, D. N.; Schneider, H. H.; Kehr, W.; Andrews, J. S.; Rettig, K.-J.; Turski, L.; Schmiechen, R.; Turner, J. D.; Jensen, L. H.; Petersen, E. N.; Honore, T.; Bondo Hansen, J. Abecarnil, a Metabolically Stable, Anxiolytic β -Carboline Acting at Benzodiazepine Receptors. *J. Pharmacol. Exp. Ther.* **1990**, *253*, 334–343. (b) Turski, L.; Stephens, D. N.; Jensen, L. H.; Petersen, E. N.; Meldrum, B. S.; Patel, S.; Bondo Hansen, J.; Loscher, W.; Schneider, H. H.; Schmiechen, R. Anticonvulsant Action of the β -Carboline Abecarnil: Studies in Rodents and Baboon. *Papio papio. J. Pharmacol. Exp. Ther.* **1990**, *253*, 344–352. (c) Ballenger, J. C.; McDonald, S.; Noyes, R.; Rickels, K.; Sussman, N.; Woods, S.; Patin, J.; Singer, J. The First Double-Blind, Placebo-Controlled Trial of a Partial Benzodiazepine Agonist Abecarnil (ZK 112-119) in Generalized Anxiety Disorder. *Psychopharmacol. Bull.* **1991**, *27*, 171–179.
- (6) (a) Pieri, L.; Hunkeler, W.; Jauch, R.; Merz, W. A.; Roncari, G.; Timm, U. Ro 16-6028. *Drugs Future* **1988**, *13*, 730–735. (b) Haefely, W.; Martin, J. R.; Schoch, P. Novel Anxiolytics That Act as Partial Agonists at Benzodiazepine Receptors. *Trends Pharmacol. Sci.* **1990**, *11*, 452–456.
- (7) Morimoto, Y.; Fukuda, T.; Yakushiji, T.; Takehara, S.; Anami, K.; Yamamoto, Y.; Yasumatsu, H.; Nakao, T.; Setoguchi, M.; Tahar, T. Anxiolytic Properties of Y-23684, a Benzodiazepine Receptor Partial Agonist in Comparison with Diazepam. Proc. 17th CINP Congr., Kyoto, 1990; Abstr. P-12-2-9, p 169.
- (8) George, P.; Rossey, G.; Depoortere, H.; Mompon, B.; Allen, J.; Wick, A. Imidazopyridines: Towards Novel Hypnotic and Anxiolytic Drugs. *Farmacol.* **1991**, *46* (suppl.), 277–288.

- (9) (a) Tang, A. H.; Franklin, S. R.; Himes, C. S.; Ho, P. M. Behavioral Effects of U-78875, a Quinoxalinone Anxiolytic with Potent Benzodiazepine Antagonist Activity. *J. Pharmacol. Exp. Ther.* **1991**, *259*, 248–254. (b) Petke, J. D.; Im, H. K.; Im, W. B.; Blakeman, D. P.; Pregenzer, J. F.; Jacobsen, E. J.; Hamilton, B. J.; Carter, D. B. Characterization of Functional Interactions of Imidazoquinoxaline Derivatives with Benzodiazepine- γ -Aminobutyric Acid_A Receptors. *Mol. Pharmacol.* **1992**, *42*, 294–301.
- (10) Maryanoff, B. E.; Ho, W.; McComsey, D. F.; Reitz, A. B.; Grous, P. P.; Nortey, S. O.; Shank, R. P.; Dubinsky, B.; Taylor, R. J.; Gardocki, J. F. Potential Anxiolytic Agents. Pyrido[1,2-a]benzimidazoles: A New Structural Class of Ligands for the Benzodiazepine Binding Site on GABA-A Receptors. *J. Med. Chem.* **1995**, *38*, 16–20.
- (11) (a) Pritchett, D. B.; Sontheimer, H.; Shivers, B. D.; Ymer, S.; Kettenmann, H.; Schonfield, P. R.; Seeburg, P. H. Importance of a Novel GABA_A Receptor Subunit for Benzodiazepine Pharmacology. *Nature* **1989**, *338*, 582–585. (b) Pritchett, D. B.; Seeburg, P. H. γ -Aminobutyric Acid Type A Receptor Point Mutation Increases the Affinity of Compounds for the Benzodiazepine Site. *Proc. Natl. Acad. Sci. U.S.A.* **1991**, *88*, 1421–1425.
- (12) (a) Skolnick, P.; Wong, G. In *Imidazopyridines in Anxiety Disorders: A Novel Experimental and Therapeutic Approach*; Zivkovic, B., Langer, S., Bartholini, G., Eds.; Raven Press: New York, 1992. For a recent review, see: Yeh, H. H.; Grigorenko, E. V. Deciphering the Native GABA_A Receptor: Is There Hope? *J. Neurosci. Res.* **1995**, *41*, 567–571.
- (13) Jacobsen, E. J.; TenBrink, R. E.; Stelzer, L. S.; Belonga, K. L.; Carter, D. B.; Im, H. K.; Im, W. B.; Sethy, V. H.; Tang, A. H.; VonVoigtlander, P. F.; Petke, J. D. High Affinity Partial Agonist Imidazo[1,5-a]quinoxaline Amides, Carbamates and Ureas at the GABA_A/Benzodiazepine Receptor Complex. *J. Med. Chem.* **1996**, *39*, 158–175.
- (14) Ulrich, R. G.; Cramer, C. T.; Bacon, J. A.; Funk, G. M.; Hunt, C. E.; Kholmukhamedov, E.; Petrella, D. K.; Sun, E. L. Interference with Hepatocellular Metabolism by a Quinoxalinone Anxiolytic and Its Carboxylic Acid Metabolite: What Factors Contribute Towards Cell Death? 1994 Annual Society of Toxicology Meeting, Dallas, TX, Mar. 14–17, 1994.
- (15) Jacobsen, E. J.; Stelzer, L. S.; Belonga, K. L.; Carter, D. B.; Im, W. B.; Sethy, V. H.; Tang, A. H.; VonVoigtlander, P. F.; Petke, J. D. 3-Phenyl Substituted Imidazo[1,5-a]quinoxalin-4-ones and Imidazo[1,5-a]quinoxaline Ureas Which Have High Affinity at the GABA_A/Benzodiazepine Receptor Complex. *J. Med. Chem.* **1996**, *39*, 3820–3836.
- (16) TenBrink, R. E.; Im, W. B.; Sethy, V. H.; Tang, A. H.; Carter, D. B. Antagonist, Partial Agonist, and Full Agonist Imidazo[1,5-a]quinoxaline Amides and Carbamates Acting through the GABA_A/Benzodiazepine Receptor. *J. Med. Chem.* **1994**, *37*, 758–768.
- (17) Borch, R. F.; Bernstein, M. D.; Durst, H. D. The Cyanoborohydride Anion as a Selective Reducing Agent. *J. Am. Chem. Soc.* **1971**, *93*, 2897–2904.
- (18) (a) Imbach, J. L.; Katritzky, A. R.; Kolinski, R. A. The Conformational Analysis of Heterocyclic Systems. Part VIII. Kinetics of Quaternisation of *N*-Alkylpiperidines and *N*-Alkylpiperazines in Acetonitrile. *J. Chem. Soc. B* **1966**, 556–562. (b) Cook, M. J.; Jones, R. A. Y.; Katritzky, A. R.; Moreno Manas, M.; Richards, A. C.; Sparrow, A. J.; Trepanier, D. L. The Conformational Analysis of Saturated Heterocycles. Part XLIX. The Conformation of Ring NH-Groups in Piperazines, Hexahydropyrimidines, Tetrahydro-1,3-oxazines, and Tetrahydro-1,3-thiazines. *J. Chem. Soc., Perkin II* **1973**, 325–331.
- (19) Braish, T. F.; Fox, D. E. Synthesis of (*S,S*)- and (*R,R*)-2-Alkyl-2,5-diazabicyclo[2.2.1]heptanes. *J. Org. Chem.* **1990**, *55*, 1684–1687.
- (20) (a) Cignarella, G.; Nathansohn, G. Bicyclic Homologues of Piperazine. Synthesis of 8-Methyl-3,8-diazabicyclooctanes. I. *J. Org. Chem.* **1961**, *26*, 1500–1504. (b) Cignarella, G.; Nathansohn, G.; Occelli, E. Bicyclic Homologues of Piperazine. II. Synthesis of 3,8-Diazabicyclo[3.2.1]octane. New Synthesis of 8-Methyl-3,8-diazabicyclo[3.2.1]octane. *J. Org. Chem.* **1961**, *26*, 2747–2751. (c) Blackman, S. W.; Baltzly, R. The Synthesis of 3,8-Diazabicyclo[3.2.1]octane and Some of Its *N*-Substituted Derivatives. *J. Org. Chem.* **1961**, *26*, 2750–2755.
- (21) Aspinall, S. R. A Synthesis of Monoketopiperazines. *J. Am. Chem. Soc.* **1940**, *62*, 1202–1204.
- (22) Ishiguro, T.; Matsumura, M. Synthesis of Piperazines. VIII. Synthesis of α (*trans*)- and β (*cis*)-2,3-Dimethylpiperazines. *Yakugaku Zasshi* **1958**, *78*, 229–231.
- (23) Yoshioka, T.; Mori, E.; Murayama, K. Studies on Stable Free Radicals. XIII. Synthesis and ESR Spectral Properties of Hindered Piperazine *N*-Oxyls. *Bull. Chem. Soc. Jpn.* **1972**, *45*, 1855–1860.
- (24) Sudo, R.; Ichihara, S. Reactions of Alicyclic Aminonitrile. *Bull. Chem. Soc. Jpn.* **1963**, *36*, 34–37.
- (25) (a) Mickelson, J. W.; Belonga, K. L.; Jacobsen, E. J. Asymmetric Synthesis of 2,6-Methylated Piperazines. *J. Org. Chem.* **1995**, *60*, 4177–4183. (b) Mickelson, J. W.; Jacobsen, E. J. Asymmetric Synthesis of (2*R*,6*R*) and (2*S*,6*S*)-2,6-Dimethylpiperazine. *Tetrahedron: Asymmetry* **1995**, *6*, 19–22.
- (26) Mitsunobu, O. The Use of Diethyl Azodicarboxylate and Triphenylphosphine in Synthesis and Transformation of Natural Products. *Synthesis* **1981**, 1–28.
- (27) The ratio of enantiomers was determined by HPLC analysis of either the amine or Mosher⁵² amide using a Chiralpak AD column (Daicel Chem. Ind., no. 53-45-20622) eluting with 30% ^tPrOH/hexane or by ¹H NMR analysis of the Mosher amide.
- (28) Sethy, V. H.; Harris, D. W. Determination of Biological Activity of Alprazolam, Triazolam and Their Metabolites. *J. Pharm. Pharmacol.* **1982**, *34*, 115–116.
- (29) Carter, D. B.; Thomsen, D. R.; Im, W. B.; Lennon, D. J.; Ngo, D. M.; Gale, W.; Im, H. K.; Seeburg, P. H.; Smith, M. W. Functional Expression of GABA_A Chloride Channels and Benzodiazepine Binding Sites in Baculovirus Infected Insect Cells. *Bio/Technology* **1992**, *10*, 679–681.
- (30) Hamilton, B. J.; Lennon, D. J.; Im, H. K.; Im, W. B.; Seeburg, P. H.; Carter, D. B. Stable Expression of Cloned Rat GABA_A Receptor Subunits in a Human Kidney Cell Line. *Neurosci. Lett.* **1993**, *153*, 206–209.
- (31) (a) Pritchett, D. B.; Seeburg, P. H. γ -Aminobutyric Acid_A Receptor α_5 -Subunit Creates Novel Type II Benzodiazepine Receptor Pharmacology. *J. Neurochem.* **1990**, *54*, 1802–1804. (b) Pritchett, D. B.; Luddens, H.; Seeburg, P. H. Type I and Type II GABA_A-Benzodiazepine Receptors Produced in Transfected Cells. *Science* **1989**, *245*, 1389–1392.
- (32) Luddens, H.; Pritchett, D. B.; Kohler, M.; Killisch, I.; Keinanen, K.; Monyer, H.; Sprengel, R.; Seeburg, P. H. Cerebellar GABA_A Receptor Selective for a Behavioral Alcohol Antagonist. *Nature* **1990**, *346*, 648–651.
- (33) Im, W. B.; Blakeman, D. P. Correlation Between γ -Aminobutyric Acid_A Receptor Ligand-Induced Changes in *tert*-Butylbicyclophosphoro[³⁵S]thionate Binding and ³⁶Cl⁻ Uptake in Rat Cerebrocortical Membranes. *Mol. Pharmacol.* **1991**, *39*, 394–398.
- (34) Schwartz, R. D.; Suzdak, P. D.; Paul, S. M. γ -Aminobutyric Acid (GABA)- and Barbiturate-Mediated ³⁶Cl⁻ Uptake in Rat Brain Synaptosomes: Evidence for Rapid Desensitization of the GABA Receptor-Coupled Chloride Ion Channel. *Mol. Pharmacol.* **1986**, *30*, 419–426.
- (35) Im, H. K.; Im, W. B.; Hamilton, B. J.; Carter, D. B.; VonVoigtlander, P. F. Potentiation of GABA-induced Chloride Currents by Various Benzodiazepine Site Agonists with $\alpha_{1\gamma/2}$, $\beta_{2\gamma/2}$ and $\alpha_{1\beta_{2\gamma/2}}$ Subtypes of Cloned GABA_A Receptors. *Mol. Pharmacol.* **1993**, *44*, 866–870.
- (36) Puia, G.; Vicini, S.; Seeburg, P. H.; Costa, E. Influence of Recombinant γ -Aminobutyric Acid_A Receptor Subunit Composition on the Action of Allosteric Modulators of γ -Aminobutyric Acid_A-Gated Cl⁻ Currents. *Mol. Pharmacol.* **1991**, *39*, 691–696.
- (37) Rudzik, A. D.; Hester, J. B.; Tang, A. H.; Straw, R. N.; Friis, W. Triazolobenzodiazepines, A New Class of Central Nervous System-Depressant Compounds. In *The Benzodiazepines*; Garattini, S.; Mussini, E.; Randall, L. O., Eds.; Raven Press: New York, 1973; pp 285–297.
- (38) Kyburz, E. Serendipity in Drug Discovery. The Case of BzR Ligands. *Il Farmaco*, **1989**, *44*, 345–382.
- (39) Im, H. K.; Im, W. B.; Pregenzer, J. F.; Carter, D. B.; Jacobsen, E. J.; Hamilton, B. J. Characterization of U-97775 as a GABA_A Receptor Ligand of Dual Functionality in Cloned Rat GABA_A Receptor Subtypes. *Brit. J. Pharmacol.* **1995**, *115*, 19–24.
- (40) (a) Sethy, V. H.; Francis, J. W.; Elfring, G. Onset and Duration of Action of Benzodiazepines as Determined by Inhibition of (³H)-Flunitrazepam Binding. *Drug Dev. Res.* **1987**, *10*, 117–121. (b) Sethy, V. H.; Daenzer, C. L.; Russell, R. R. Interaction of *N*-Alkylaminobenzophenones with Benzodiazepine Receptors. *J. Pharm. Pharmacol.* **1983**, *35*, 194–195.
- (41) (a) Dinnendahl, V. Effect of Stress on Mouse Brain Cyclic Nucleotide Levels In Vivo. *Brain Res.* **1975**, *100*, 716–719. (b) Dinnendahl, V.; Gumulka, S. W. Stress-induced Alterations of Cyclic Nucleotide Levels in Brain: Effect of Centrally Acting Drugs. *Psychopharmacology* **1977**, *52*, 243–249. (c) Goldberg, N. D.; Haddox, M. K.; Hartle, D. K.; Hadden, J. W. The Biological Role of Cyclic 3',5'-Guanosine Monophosphate. In *Pharmacology and the Future of Man*; Maxwell, R. A., Acheson, G. H., Eds.; Karger: Basel, 1972; pp 146–169.
- (42) Sethy, V. H.; Oien, T. T. Role of cGMP in the Mechanism of Anxiolytic Activity of U-78875. *Pharmacol. Biochem. Behavior.* **1991**, *39*, 379–382.
- (43) (a) VonVoigtlander, P. F.; Lewis, R. A. A Rapid Screening Method for the Assessment of Benzodiazepine Receptor-Related Physical Dependence in Mice. *J. Pharmacol. Methods* **1991**, *26*, 1–5. (b) Fialip, J.; Aumaitre, O.; Eschaliere, A.; Maradeix, B.; Dordain, G.; Lavarenne, J. Benzodiazepine Withdrawal Seizures: Analysis of 48 Case Reports. *Clin. Neuropharmacol.* **1987**, *10*, 538–544.

- (44) Mohamadi, F.; Richards, N. G. J.; Guida, W. C.; Liskamp, R.; Lipton, M.; Caufield, C.; Chang, G.; Hendrickson, T.; Still, W. C. MacroModel-An Integrated Software System for Modeling Organic and Bioorganic Molecules Using Molecular Mechanics. *J. Comput. Chem.* **1990**, *11*, 440–467.
- (45) Weiner, S. J.; Kollman, P. A.; Nguyen, D. T.; Case, D. A. An All Atom Force Field for Simulations of Proteins and Nucleic Acids. *J. Comput. Chem.* **1986**, *7*, 230–252.
- (46) Allinger, N. L. Conformational Analysis. 130. MM2. A Hydrocarbon Force Field Utilizing V_1 and V_2 Torsional Terms. *J. Am. Chem. Soc.* **1977**, *99*, 8127–8134.
- (47) Chang, G.; Guida, W. C.; Still, W. C. An Internal Coordinate Monte Carlo Method for Searching Conformational Space. *J. Am. Chem. Soc.* **1989**, *111*, 4379–4386.
- (48) Stewart, J. J. P. MOPAC, A Semiempirical Molecular Orbital Program. *J. Comput.-Aided Mol. Des.* **1990**, *4*, 1–105.
- (49) Dewar, M. J. S.; Zoebisch, E. G.; Healy, E. F.; Stewart, J. J. P. AM1: A New General Purpose Quantum Mechanical Molecular Model. *J. Am. Chem. Soc.* **1985**, *107*, 3902–3909.
- (50) Tebib, S.; Bourguignon, J.-J.; Wermuth, C.-G.; The Active Analogue Approach Applied to the Pharmacophore Identification of Benzodiazepine Receptor Ligands. *J. Comput.-Aided Mol. Des.* **1987**, *1*, 153–170.
- (51) Zhang, W.; Koehler, K. F.; Zhang, P.; Cook, J. M. Development of a Comprehensive Pharmacophore Model for the Benzodiazepine Receptor. *Drug Des. Discovery* **1995**, *12*, 193–248.
- (52) Dale, J. A.; Mosher, H. S. Nuclear Magnetic Resonance Enantiomer Reagents. Configurational Correlations via Nuclear Magnetic Resonance Chemical Shifts of Diastereomeric Mandelate, *O*-Methylmandelate, and α -Methoxy- α -trifluoromethylphenylacetate (MTPA) Esters. *J. Am. Chem. Soc.* **1973**, *95*, 512–519.
- (53) Burkard, W. P.; Bonetti, E. P.; Haefely, W. The Benzodiazepine Antagonist Ro 15-1788 Reverses the Effect of Methyl- β -carboline-3-carboxylate but not of Harmaline on Cerebellar cGMP and Motor Performance in Mice. *Eur. J. Pharmacol.* **1985**, *109*, 241–247.
- (54) Waynforth, H. B. In *Experimental and Surgical Technique in the Rat*; Academic Press: London, 1980; pp 50–57, 72–74.
- (55) Gibaldi, M.; Perrier, D. In *Pharmacokinetics*, 2nd ed.; Swarbrick, J., Ed.; Marcel Dekker: New York, 1982; pp 5, 411.

JM9801307